Solar Energy Driven Microfluidic Reactor for Continuous Production of Syngas by CO_2 Reduction

BY

DAVIDE PISASALE
B.S., Politecnico di Torino, Turin, Italy, 2011

THESIS

Submitted as partial fulfillment of the requirements
for the degree of Master of Science in Mechanical Engineering
in the Graduate College of the
University of Illinois at Chicago, 2013

Chicago, Illinois

Defense Committee:

    Amin Salehi-Khojin, Chair and Advisor
    Marco Carlo Masoero, Politecnico di Torino
    Kenneth Brezinsky

To my mother and father,
to Fede, Raffa and Leo, joy of life,
to my sisters and brothers,
and to my friends.

ACKNOWLEDGMENTS

This thesis paper could not be written without Dr. Salehi, who served as my supervisor, gave me support and assistance, and provided me motivations and encouragement throughout the entire period of my research work at the Nanomaterials and Energy Systems Laboratory. My deepest gratitude goes also to my advisor at Politecnico di Torino, Dr. Masoero, who gave me the possibility to undertake this research work at UIC. I wish also to thank Mohammad, Narbeh, Tyler and Misagh who helped me complete this dissertation.

TABLE OF CONTENTS

TABLE OF CONTENTS (continued)

CHAPTER   **PAGE**

LIST OF TABLES

LIST OF FIGURES

SUMMARY

The anthropogenic emissions of carbon dioxide (CO_2) and other greenhouse gases (GHGs) into the atmosphere have been exponentially increasing since the industrial revolution, and have been recently recognized as the main cause of ongoing climate change. Predictions of possible future scenarios suggest that various routes for GHG emissions reduction must be undertaken, including progressive shifts from traditional fossil fuels to green, renewable, carbon-free energy generation technologies. Additionally, carbon-capture systems would represent a significant tool for stabilizing current atmospheric CO_2 concentration. Captured CO_2 can be subsequently recycled (e.g. for enhanced oil recovery) or converted into high-energy density chemicals, outlining a potential flexible approach for storing excess energy produced by renewable energy sources. Electrochemical reduction of CO_2 has been recently recognized as a strong candidate to perform CO_2-to-fuel conversion at favorable energy efficiencies. Nonetheless, the development of a cost-effective catalytic system that would perform the conversion at a low-overpotential, high current efficiency (faradaic efficiency), and high conversion rate (current density), remains a challenge. This paper proposes a low-cost co-catalytic system which exhibits exceptional performance - i.e. negligible overpotential, nearly 100% current efficiency, and the greatest current density reported thus far - for electrochemical CO_2 reduction. The integration of the system in a microfluidic-type reactor - powered by a solar panel - provides promising results for effective continuous CO_2 conversion to syngas fuel.

CHAPTER 1

INTRODUCTION

1.1   Carbon dioxide and the carbon cycle

Carbon dioxide (CO_2) is the fourth most abundant gas in earth's atmosphere, after Oxygen, Nitrogen, and Argon; however, it is arguably the most important substance in the biosphere. As part of the Carbon Cycle, the great natural recycler of carbon atoms, CO_2 serves as the main source of carbon, and has supported the development and existence of life. Additionally, its presence in air is responsible for the natural acidity (pH 5.7) of precipitation [1]. A detailed understanding of how the Carbon Cycle operates will elucidate the often detrimental effect human activity has on the global climate. For these reasons, interest in research related to the Carbon Cycle has intensified, as it undertakes some of the most important scientific challenges of this century.

The carbon cycle can be theoretically split into a biologically-mediated (organic) process, or a non-biologically-mediated (inorganic) one. In the former, algae, plants, and other "producers" absorb carbon dioxide from the surrounding air or water through the biochemical reaction of photosynthesis,

$$6CO_2 \; + \; 6H_2O \; + \; light\ energy \; \rightarrow \; C_6H_{12}O_6 \; + \; 6O_2.$$
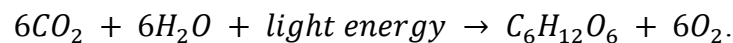
Energy-rich sugar is formed, stored, and used by the producers themselves to continue performing the biological activities and, simultaneously, oxygen is released into the atmosphere as a byproduct. Animals, bacteria, fungi, and other "consumers" feed upon the "producers" (or other "consumers" that have ingested "producers") obtaining carbon from them. In the reverse reaction, carbon dioxide and water return to the environment during respiration and decomposition of living organisms. Carbon fixation during photosynthesis and the process of respiration are always in equilibrium with each other; and they constitute the organic part of the carbon cycle. It's noteworthy that a portion of the total organic carbon is not directly released into the atmosphere; in fact, it collects in various sinks such as swamps, lake bottoms, or seafloors. The stored carbon accumulates and eventually becomes trapped in deposits of sediment and over hundreds of millions of years it segregates in the Earth's crust in the form of coal deposits; alternatively, it accumulates in ocean floors as hydrocarbons, oils, and natural gases.

The inorganic Carbon Cycle utilizes the carbon that does not take part in the organic cycle, thus making the inorganic cycle independent of biochemical processes. It mainly consists of the carbon involved in the dissolution of carbon dioxide in water and hence stored in the oceans and finally, considering a long-time period, in the geosphere. We distinguish two main processes through which the carbon covers this pathway [2]. The first is called the 'solubility pump', and takes into consideration the circulating currents in the ocean. Briefly explained, due to the combination of winds, Earth rotation

and the restriction on movements of water caused by shorelines, cold and dense water at the surface (rich of CO_2 because of higher solubility) converges to the bottom, sinking carbon (downwelling phenomenon). In the reverse process, carbon can eventually return back to the atmosphere when the deep ocean water is driven toward the surface (upwelling).

The second is the 'hydrolysis' chemical reaction. It is an irreversible chemical weathering reaction that involves the formation of carbon acid in rainwater and in groundwater and its subsequent hydrolysis with silicate minerals. The products of this reaction will either accumulate in soil (sedimentary depositing) or they will be streamed into the oceans through the groundwater, where they react again forming carbonate mineral. Hence, carbon dioxide is removed from the atmosphere, buried in the limestone rock, and can persist in the crust of the Earth for hundreds of millions of years. In the reverse process that completes the cycle, carbon sediments can be pushed into the Earth's mantle and be subjected to metaphormism at extremely high temperature and CO_2 can ultimately return back to the atmosphere during volcanic eruptions.

The 'biological pump' acting as part of the organic cycle, the 'solubility pump', and more generally the transformation and circulation of carbon back and forth from the environment to the living things evinces a dynamic characteristic that is fundamental for climate regulation on our planet, tying together the functioning of the Earth's atmosphere, oceans, geosphere and biosphere.

1.2   <u>Anthropogenic carbon emissions: climate change</u>

If the carbon cycle maintains equilibrium between the carbon in the atmosphere and the carbon stored in the crust of the Earth, why the amount of CO_2 in the air is increasing dangerously nowadays?

Burning fossil fuels (mainly for electricity generation in power plant and to feed the transportation system), we basically draw upon the sedimentary organic carbon deposits, that is the carbon removed from the atmosphere over hundreds millions of years, and we send it back to the atmosphere in the form of CO_2 at a rate of several gigatonnes per year [3]. In other words we are manipulating and destabilizing the natural equilibrium, releasing in the air an enormous volume of carbon dioxide in an extremely short time compared to how long would need to the geological processes to bury it back into the crust of the Earth. According to the geochemists, lands and oceans carbon reservoirs are taking up half of the CO_2 emission (exactly 55%) [4,5], and they would be able to absorb up to 90% of the CO_2 liberated by our industrializing world, but in a natural process that works too slowly for a human time scale [2]. Furthermore, the continue increment of the concentration of carbon dioxide in the atmosphere and the consequent climate variability have changed the sink fluxes operated by lands and oceans, and some models predict a decay in the uptake of carbon by these storage sources, resulting in a 'stronger-than-expected' and a 'sooner-than-expected' climate forcing [6].

1.2.1   <u>Greenhouse Effect</u>

In order to understand how the rapid and excessive 'injection' of CO_2 into the atmosphere turns to be dangerous for our planet climate, it is significantly necessary to mark the connection that occurs between carbon cycle, atmosphere and climate change.

Earth atmosphere is mainly composed by Nitrogen (78.08%) and Oxygen (20.95%), and in smaller percentages by other gases (Water vapor, Argon, Carbon Dioxide, Neon, Helium, Methane, Hydrogen, Nitrous Oxide and Ozone). Some of these gases present in minor quantities are responsible for the so-called greenhouse effect: "a naturally occurring phenomenon wherein certain atmospheric gases, such as Water vapor, Carbon Dioxide - and Methane - regulate the radiant energy balance of Earth, thus making it habitable" [7]. The radiation emitted by the sun is in the form of shortwave radiation in the ultraviolet and visible portions of the spectrum. The 70% of this radiation pass through the atmosphere and it is absorbed by Earth surface and reflected back in the form of longer-wavelength infrared radiation. Greenhouse gases (GHGs) are opaque to infrared radiation and therefore, even if they are present in relatively small quantities, they trap most of the radiant heat re-emitted by the Earth surface readily absorbing it and avoiding its escaping back into space and in consequence warming the atmosphere and keeping it at an average temperature adequate for life on Earth (15 °C compared to -18 °C estimated average global temperature without the greenhouse effect).
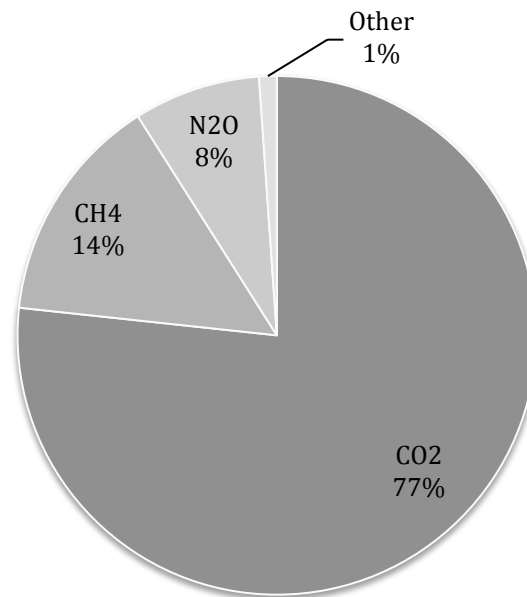
Figure 1. Share of different GHGs in total emission by human activities in 2004 [8].

Unfortunately, even if they represent a very small portion of the total gases in the atmosphere, they have a disproportionate influence on its energy equilibrium with effects on global warming and climate change, and this explains the reason for a common concern on the on-going increase in GHG concentration in the atmosphere induced by human activities. Moreover, forced global warming results in a positive feedback (a warmer Earth causes an increase in the evaporation and therefore in the concentration of water vapor in the atmosphere) that dangerously leads to further warming. According to some NASA scientists the warmer average temperature induced by greenhouse effect can hasten a climate catastrophe due to a brand new feedback loop recently discovered: an

enormous amount of GHGs is trapped in the frozen tundra across Siberia, Alaska and Canada, and the melting of permafrost due to the ongoing Earth warming could eventually contribute to an additional 35% of worldwide GHG emission in a relatively short-time period [9]. Must also be taken into account that greenhouse effect is not the only factor responsible for climate change. Some recent studies show in details how fluctuation of the Sun luminosity influences the average temperature of the Earth in both short-term and long-term periods [10,11]. Finally pyroclastic eruptions subsequent to tectonic plate collisions, flood basal eruptions and in general volcanic activity can emit large amounts of CO_2 driving climate change over a variety of time-scales.

1.2.2 Greenhouse gases emissions and global warming

The first alarm bell on the risk that an increase in atmospheric carbon dioxide concentration would lead to a warmer planet was given early in the 1895 by the chemist Svante Arrenhius [12]. His concerns were right, and as time went by, the exponentially rise in the anthropogenic CO_2 emissions and the resulting accelerated rate of global climate warming have became of principal interest and concern for scientists, governments (see Kioto Protocol for reduction of GHGs) and finally for public opinion, in an ongoing favorable investigation on causes and possible catastrophic effects for human life.

A further confirmation of the dangerous connection that occurs between anthropogenic GHG emission comes from the fourth assessment report redacted in 2007 by the Intergovernmental Panel of Climate Change, the leading international body for the assessment of climate change: "*Most of the observed increase in global average temperatures since the mid-20th century is very likely due to the observed increase in anthropogenic greenhouse gas concentrations*". Where, with 'very likely', a 90% probability must be intended.

1.2.3 <u>Atmospheric CO_2 concentration. Sources and sinks</u>

At the start of industrial revolution ($\approx$1750) the concentration of CO_2 in the air was around 280 ppm. As in February 2013 it has reached the value of 396.80 ppm [13], probably the highest in the last 20 millions years [14]. Moreover, since 1958, that is since it has been constantly monitored, the annual mean carbon dioxide growth rate (ppm/yr) has risen from 0.94 ppm/yr (1959) to 2.67 ppm/yr (2012) as it is showed in Figure 2, with an average of 2.11 ppm of increase every year in the last decade.
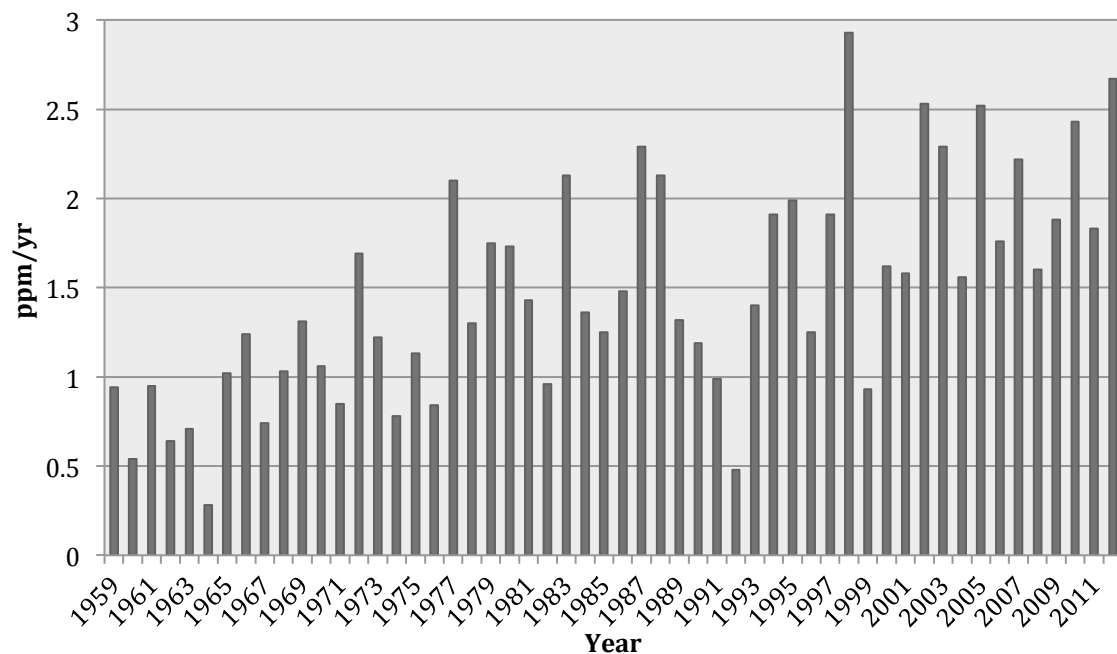
Figure 2. Annual mean growth rate of CO_2 since it has been monitored at Mauna Loa

Observatory, Hawaii [13]

It has been estimated that from 1750 to 2000, more than 350 PgC (1 PgC = 10^9 metric tons of carbon) have been released to the atmosphere due to the fossil-fuels combustion, cement production, and land-use change. In Figure 3 it is shown the exact CO_2 emissions sources share composition from 1959 to 2011. Only in 2011 a total amount of 9.5 PgC (or rather 34.7 billions of metric tons of CO_2) have been injected into the atmosphere, that corresponds to a 54% increase with respect to global emissions on 1990 (Tokyo Protocol year of reference). Of this enormous volume of CO_2 emitted into

the atmosphere, China is responsible for a quarter of the total, how it can be seen on Figure 4. United States emissions contribution follows at 17 % and at the third place India with its 7 %.
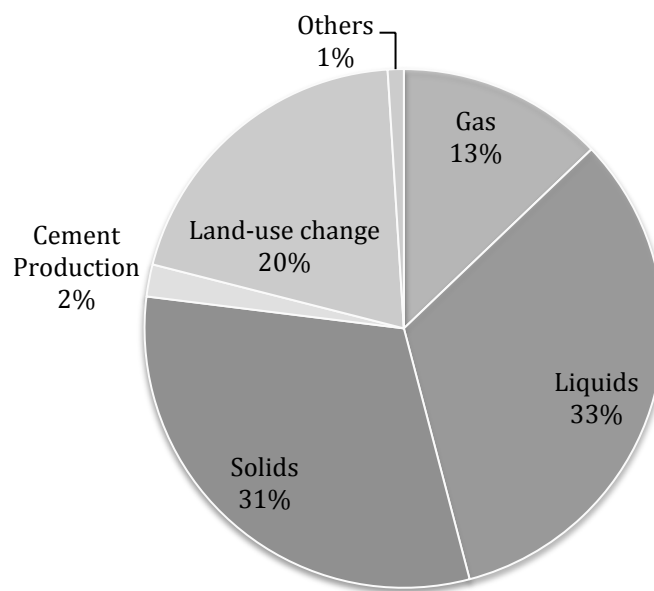
Figure 3. Global CO_2 Emissions from solid, liquid and gas fossil-fuel burning, cement manufacture, land-use change, and others (as gas flaring): from 1959-2011 [15].

Electricity generation is the main source of global CO_2 emission from fossil-fuels burning. In the United States it represents the 38.5% of total carbon dioxide emitted in

recent years, and it contributes for 32% of the total GHG emission. At a global scale, the contribution from energy supply drops down to 25.9% (2004) [8]. Industry is the second source representing the 19.4% of total GHG emitted by human's activities. Transportation follows at 13.1 %, but if we consider only the U.S., it is the second sector contributing for nearly 26% of GHG emission (industry in the U.S. steps back at 11.4%). Finally emissions from residential and commercial building represent the 7.9% of global GHGs.
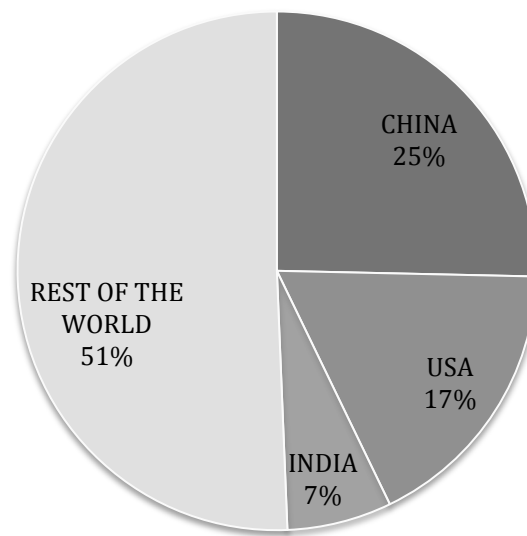
Figure 4. Share of the 2009 total CO_2 emissions by countries [15].

It can be interesting remark how the results look totally different if we connect the CO_2 emission of the country to its actual population. In Figure 5 the top 12 countries

in this ranking for 2009 are shown, and Qatar, with its 12 metric tons of carbon emission per capita, precede Trinidad and Tobago (9.75) and Netherland Antilles (8.44). Among the most industrialized countries United States fails its 'contend' with China: the 4.64 metric tons of carbon emission for which an US citizen was responsible for in 2009, more than doubled the 1.57 of a Chinese. The negative primate of United States in this case could be attributed to its higher number of car per capita and the consequent higher number of total miles driven by its population.
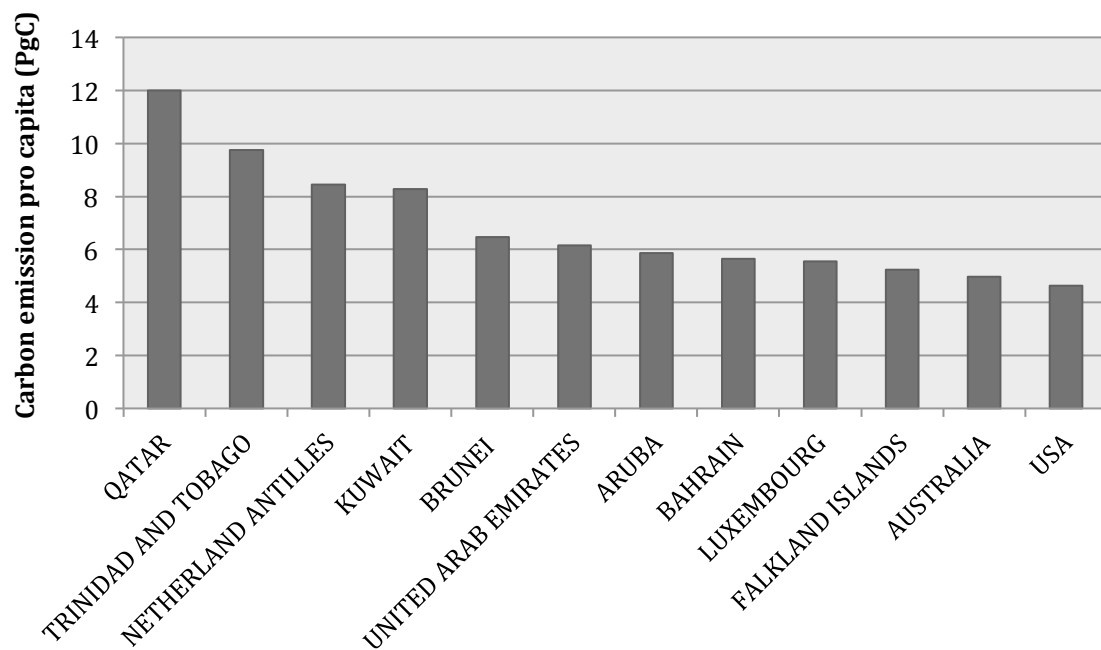
Figure 5. Top 12 countries in the ranking of the world's countries by 2009 per capita fossil-fuel CO_2 emission rates. The values are expressed in metric tons of carbon per capita [15].

Finally it is possible to couple CO_2 emission to gross world product (GWP), that is the combined gross national product of all the countries in the world. Connecting the increase in GHGs concentration to the global economic activity can be of primary interest revealing how much carbon must be released to the atmosphere to produce a unit of economic activity at global scale. Recent studies report a value of 0.35 kgC/dollar in 1970 and a declining trend down to 0.24 kgC/dollar in at the end of 20th century [16,17]. Unfortunately since 2000 this negative trend has reversed into a positive one leading to an increase of ≈0.3% every year (last report 2006). Reducing the value of the so defined "*carbon intensity of the global economy*", keeping the global emission growth rate below the global economic growth rate it is one of the biggest challenge to face in the enormous effort that must be taken to improve the future scenario of CO_2 emission, for the preservation of our planet.

1.2.4   Carbon emissions from land-use change

Combustion of fossil fuels and cement production are not the only processes contributing to CO_2 emissions. Land-use change and the already mentioned decline in the efficiency of CO_2 sinks (lands and oceans) must be taken into consideration for the estimation of the actual global carbon budget. Land-use change causes a net flux of carbon from biosphere to atmosphere and Figure 6 gives us an idea of the contribution of

carbon emission coming from deliberated changes in land cover and land use. While CO_2 emission coming from fossil-fuels burning have been increasing during last 50 years, the emissions caused by changes in land use and land management show an approximately stable trend with a slight decay on the last decade.
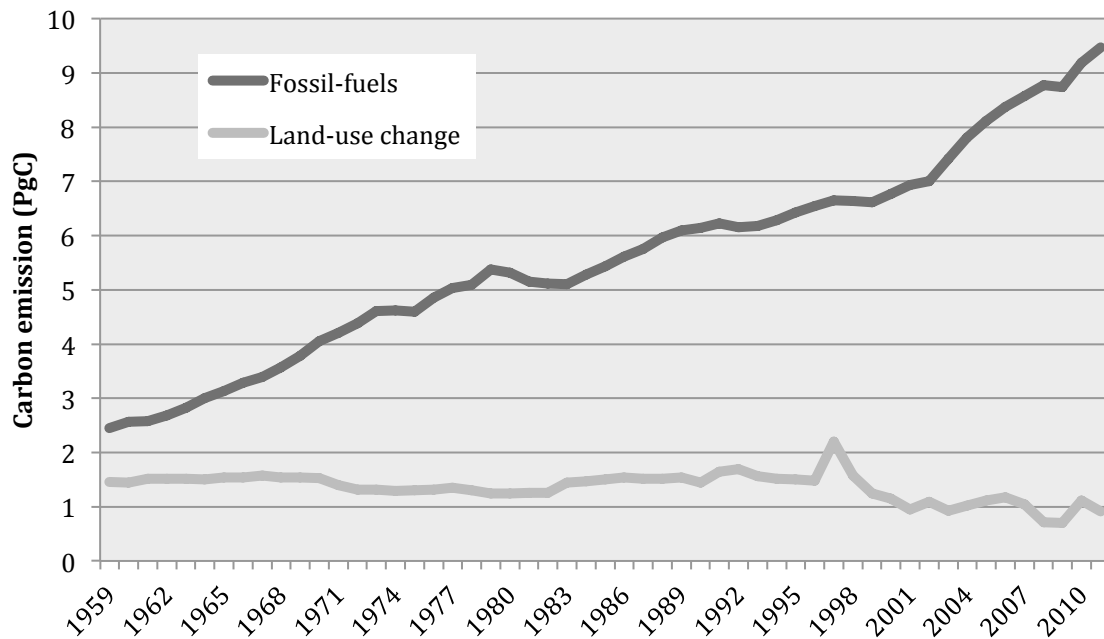
Figure 6. Trends of fossil-fuels burning and land-use change emissions of CO_2 from 1959 to 2011 [15].

If we consider the cumulative net flux of carbon dioxide released into the atmosphere due to this process from 1959 to 2011, as it is shown in Figure 7, land-use change is responsible for the ≈19% of the total (72.13 PgC), with an average of 1.36 PgC

injected every year. In the last decade (2001 to 2011) this process stabilized to lower values: it contributed just for ≈10% of the total CO_2 emission, with an average of 0.98 PgC per year. The estimated values take into account only the flux caused by direct human activities. These can mainly be identified by land conversion (e.g. transformation of natural ecosystem to cultivated lands), which also represents the greatest cause for extinction of terrestrial species, and deforestation. The annual flux of carbon from changes in land use and land management has a different estimate inside and outside the tropics: permanent deforestation in the tropics has accounted for 94% of the total annual loss of carbon for deforestation during the 1990s.
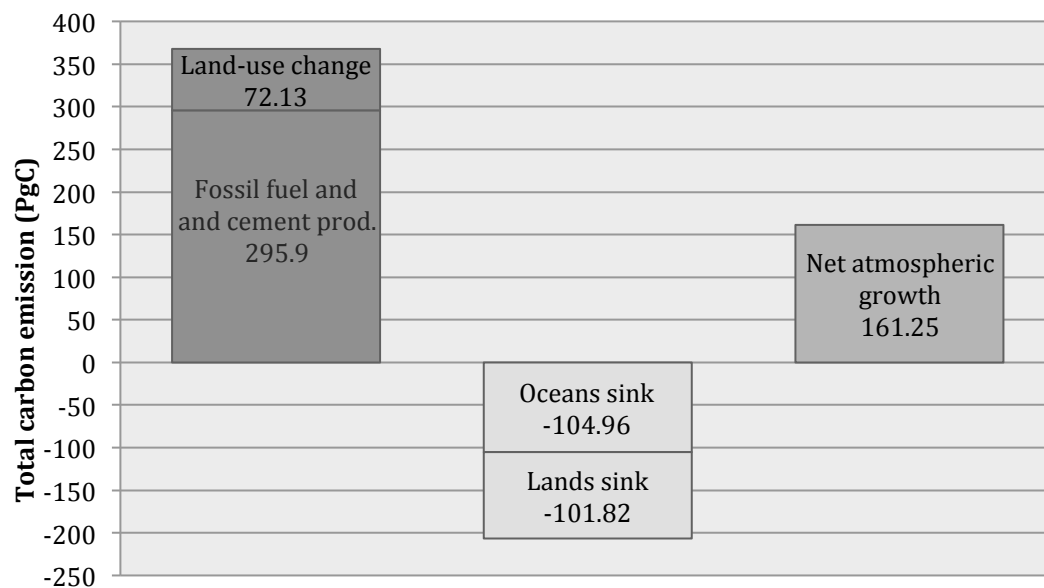
Figure 7. Estimated cumulative carbon budget from 1959 to 2011. Negative sign indicate the uptake carbon by the ocean and land sinks during this period [15].

Figure 7 shows also the amount of carbon sequestrated by natural sinks during last five decades. Oceans and lands in their natural role inside the carbon cycle have absorbed a total of 206.78 PgC that corresponds to 56% of the total carbon emission. Unfortunately, as time went by, although the size of natural sinks size have been increasing, the efficiency have been slightly declining from 60% to 55%.

In conclusion, summarizing all the data illustrated so far, and connecting them to the ongoing challenge of stabilize future CO_2 emission, it might be useful citing Canadell *et al*. work, for which the causes of the dangerous rapid increase in atmospheric CO_2 concentration of the last few decades can be found in three main factors: firstly the accelerating global economic growth (65% ± 16%), directly connected to world's dependence on fossil fuels for energy supply, increase in transportation and in the industrial production of iron and steel, changes in land-use and deforestation [16]. Secondly, in the declining efficiency of natural sinks such as oceans and land (18% ± 15%), and lastly in the increase of carbon intensity of the global economy (17% ± 7%). Mitigation of CO_2 emissions, acting as much as possible on these factors, is the challenge for stabilizing global warming trend.

1.3   Global warming: future scenarios

As already mentioned there are several evidences showing a strict connection between increase in anthropogenic greenhouse gas emissions and warming of planet climate. Although some other natural climate change mechanisms could contribute to current warming trend, a full-knowledge of the physical laws governing greenhouse gas effect, temperature measurements of troposphere and stratosphere, and computer modeling have shown that the reciprocal correlation between anthropogenic GHG emission and climate warming is unequivocal.

On last assessment report issued by the IPCC on 2007, climate change is identified by the "*changes in the mean and/or the variability of its properties, and that persists for an extended period, typically decades or longer*". Evidences of the ongoing climate change come from the increases in global average air and ocean temperatures, melting of ice and rising of sea level. In Figure 8 it is shown the upward trend of land-surface temperature from 1880 to 2012. The data from GISS Surface Temperature Analysis (NASA) are expressed in terms of 'anomalies' (temperature change with respect to a reference period), mainly because annual temperature anomalies are representative of a larger period of time compared to absolute temperatures which varies in short distance. The right vertical axis expresses the absolute temperatures taking into account that a good approximation for average temperature on the reference period (1951 – 1980 corresponding to the 'zero' anomalies) is of 14 °C. After a slight fluctuation

between 1940s and 1970s, global temperature has been sharply increasing reaching a record peak of 14.91 °C absolute mean annual temperature in 2010. An interesting, and dangerous, data comes from observation of linear trends: during the last 50 years the temperature has shown a linear upward trend of 0.02 °C per year, which doubles the linear warming trend of the last 100 years (0.01 °C/year).
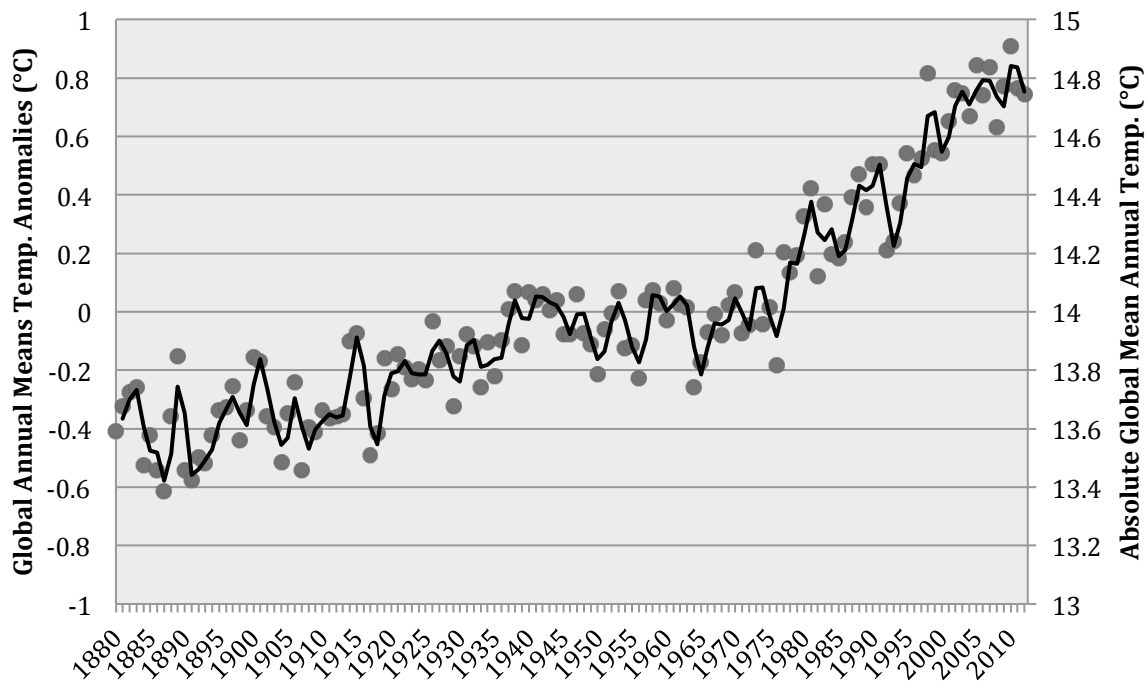
Figure 8. Anomalies and absolute values of global annual means temperature on land-surface from 1880 to 2012 [18].

Although in the last decade we have experienced some of the warmest years in the recent history of our planet, in the past Earth has been warmer than nowadays. Why should we be concerned about the ongoing warming climate change trend? Basically the answer rely on the fact that humanity has invested on the climate at it has been on the 20th century, inducing a geographical and economic dependence from it. Besides the effects on atmosphere and biosphere, the main consequence of the significant increase in temperatures on the 21st century would be the onerous adaptation of societies to the new and still uncertain scenario.

To predict future climate scenario is the main task of the IPCC, giving to policymakers the possibility to respond properly to the risks associated with a global warmer planet. The IPCC in 2000 accomplished this task publishing the Special Report on Emissions Scenarios (SRES) that was later used in the subsequent assessment reports redaction.

The SERS scenarios are shown on Figure 9, which represents the set of scenarios for GHG emissions from 2000 to 2100 in the absence of additional climate policies, expressed in $GtCO_2$-eq (gigatonnes of CO_2-equivalent) per year. They are grouped in six different alternative modeling approaches or scenario families, and, as it is remarked, "*SRES scenarios can be viewed as a linking tool that integrates qualitative narratives or stories about the future and quantitative formulations based on different formal modeling approaches*" [19]. None of the predicted scenario, then, is more likely to occur than the

others, they just represent "*possible alternative futures*" rather than "*preferred developments*".
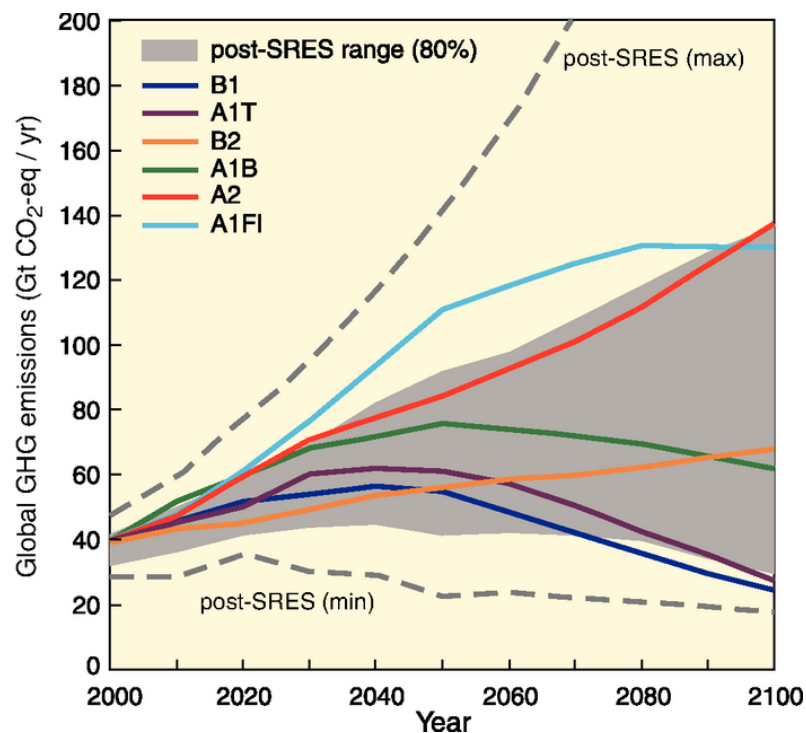
Figure 9. Global GHG emissions in $GtCO_2$-eq per year in the absence of additional climate policies. The emissions include CO_2, CH_4, N_2O and F-gases [8].

In Figure 9, the A1 scenario family takes into consideration a rapid economic growth, a global population peak of 9 billions on 2050, and introduction and spread of efficient technologies. The storyline A1FI belongs to A1 group with an emphasis on

fossil-fuels combustion (Fossil Intensive). A1T and A1B represent respectively a non-fossil energy sources and a balanced across all the sources scenario. Family B1 represents a world with the same global population trend as A1, same economic growth but with more emphasis on service and information economy. B2 is of a more ecologically friendly world, with a slower global population growth, and local solutions for the sustainability of economy, society and environment. Finally A2 is characterized by continuously increasing population but slow economic and technologic development. In the graph, the post-SRES scenarios (grey area), account for assessments studies and changes in growth models published after the first SRES reduction on 2000, resulting though in a little correction in overall emission levels.

Even if ideally the concentration of GHGs could be held constant at its value on year 2000, temperature would continue to rise of 0.6 °C (best estimate in a range from 0.3 °C to 0.9 °C) to the last decade of the twenty-first century. This represent the best scenario compared to the storylines described above, in which IPCC estimates average global temperature will likely rise by 1.8 °C to 4.0 °C in hundred years.

Many physical and biological systems are being subjected to regional climate changes and global warming. We are observing a rise in the ground stability in permafrost areas, an extension and an increase in numbers of glacial lakes, and modification in Artic and Antarctic ecosystems. Global sea level is growing dangerously (close to 10 cm than the average level registered from 1961 to 1990), and it is expected to

rise by an additional 30 to 50 cm, with consequences for large coastline regions worldwide. Moreover thermal structure and water quality is being deteriorated due to warming of lakes and rivers. The distribution of rainfall in some large world region is changing (Northern Africa and American Southwest are becoming more arid whereas United States and Canada are predicted to become wetter) with irreparable effects on agriculture systems. More heat energy in the oceans will likely intensify hurricanes and tornados occurrence. There are evident effects also on the biological system such as registered earlier timing of spring events, and 'greening' of vegetation during spring. Finally the worst effects for biosphere are those related to the extinction of species caused by local climate changes and subsequent ecosystem stresses.

The irreversibility of the effects of global warming is the main concern for Earth scientists. Even if the anthropogenic GHG emission remained constant, the planet would still experience warming for the following centuries, with its catastrophic effects on the biosphere and human life. To hold global temperature constant hence stabilizing Earth climate, near-zero future carbon emissions are required, which appears to be an utopian solution given our dependence on fossil-fuel based infrastructures.

Different pathways for GHG emission reduction must be undertaken, with adoption and implementation of policy frameworks. This includes establishment of near- mid- and long- term deadlines for progressive targets to reduce CO_2 emissions coming from power generation, transportation, industrial production of iron and cement,

residential and commercial buildings. Moreover, cooperative action is required by the developed and large emitting countries for the implementation of policy tools such us market-based incentives, government loans and investments tax credits, incentives and investments in research to develop renewable energy technologies and to improve the efficiency of the existent carbon-based infrastructures. Ultimately, research, adoption and development of methods for carbon capture and subsequent sequestration (CCS), or reutilization for conversion in useful products, represent valid local- and global-scale strategies that must be implemented in order to reach the agreed GHG emission targets.

CHPATER 2

CLIMATE CHANGE MITIGATION

2.1   Greenhouse Gases emissions reduction

Carbon Dioxide concentration in the atmosphere can be reduced by following three main pathways: adopting strategies for energy efficiency and conservation; replacing traditional energy resources with carbon-free or reduced-carbon ones; and capturing carbon either from the atmosphere or from power plants' exhaust and storing the captured carbon so that it may eventually be converted into useful products.

2.1.1   Improve energy efficiency

The application of a wide range of technologies can lead to a reduction of the amount of energy required to provide products and services, thus improving energy efficiency. A set of options and strategies are available and can be adapted in different sectors, from residential buildings to industry. It's in the heavy industry where the emissions reduction options can lead to considerable savings, via the implementation of high efficiency electric motors, process integration, energy management systems, and cogeneration of heat and power. According to an extended study conducted by the World Energy Council in 1995, replacing the existing equipment with the most efficient and

modern technologies available would, by 2020, reduce industrial energy requirements up to 70 Exajouls (EJ) per year, with respect to a baseline scenario. In terms of carbon emissions, 70 EJ of energy saving per year corresponds approximately to 1.1 PgC not emitted into the atmosphere.

On the third assessment report, the IPCC lists the most important examples of industrial energy efficiency improvement technologies that can be adopted, together with the emissions reduction potential of each (for 2010) and their associated cost [20]. The reduction potential varies among different countries and developing countries alone could account for approx. 50% of the total savings thanks to their high production growth rate. On the other hand, efficient lighting, improved insulation, and alternative design for active solar heating are examples of key technologies for energy savings in residential and commercial buildings.

2.1.2 Adopting carbon-free energy sources

Another way to reduce GHGs concentration in the atmosphere is the adoption of carbon-free energy sources. Fossil fuels supplied 80% of world's energy in 2004, and they will remain the dominant source of energy until 2030 [21]. With 160 EJ of energy produced per year (33% of total primary energy supply), oil is the largest constituent, then coal (120 EJ or 25%), and then gas (100 EJ or 21%) [8]. Unfortunately, the use of

fossil fuels was responsible for 77% of the total anthropogenic CO_2 emissions (as shown in Figure 3), making them the principal cause of the GHG effect and global warming [22].

Although renewable energy sources have their own detrimental impact due to their manufacturing processes and other minor emissions (see Figure 10) during transportation and installation, this impact is negligible when their entire life cycle is taken into consideration. Therefore, they can be thought of as carbon free sources, representing the best alternative to traditional fossil (coal, gas and oil) energy sources. As of 2004 Renewable energy sources accounted for 15% of the global primary energy supply [8]. According to the International Energy Agency (IEA), the market share is not projected to change drastically, but it will either drop to 13.7% (Reference Scenario) or increase slightly to 16.2% (Alternative Scenario) by 2030 [21]. The development of renewable sources of energy is also limited by their intermittent nature and the difficulty of integrating them into the existing electricity grid. It is clear that a strong and sustained policy intervention is needed to affect positively the projected data, toward a higher adoption of clean energy sources.

First in the list of the most productive renewable energy source is traditional biomass with 37 EJ produced and 7.6% share of total energy supply (data 2005) [8]. Energy generation by hydropower plants follows with 25 EJ and 5.1% share. Geothermal, bioethanol fuel, photovoltaic (PV) and wind represent most of the remaining

2.7% renewable energy supply share. According to the IPCC classification, the above mentioned renewable sources characterize the category "technologically mature with established markets in at least several countries"; where they have been adopted and developed to reach a competitive level in today's energy market, without the support of particular policy. The average costs ($ per MWh) of renewable energy technologies vary based on the geographical installation area, the technology development level, and the availability of resources. Except for hydropower and biomass, the average cost is still higher than in the case of traditional power generation even in an optimal scenario [23]. Large investments in the last decades, the increasing experience, and the technological development are recently inducing a significant cost reduction, making some of the most 'expensive' renewable technologies competitive for grid electricity production.

The other categories of renewable energies, according to the IPCC classification, contain mainly technologies under-development; some of which have mature markets and others with new and immature markets. Examples include municipal solid waste-to-energy, biodiesel, concentrated solar power, wave power, thin-film PV, solar thermal towers. Examples of technology in earlier stages of research include nanotechnology solar cells, artificial photosynthesis, and power from ocean currents.

Renewable energy can help separate the strong connection between rising global energy demand and GHG emission growth, making a sustainable human development feasible. The latter is possible when the needs of the present generation are satisfied

without compromising the ability of future generations to meet their needs. Social and economic development is realized together with climate mitigation, reduction of environmental impacts, and benefits on air pollution and health.

As previously mentioned, the impact on the environment due to renewable energy technologies is very small and in most of the cases comes from manufacturing, transportation and installation processes. The chart on Figure 10 shows GHG emissions of the main sources of energy for electricity generation. The values reported by the IPCC come from an aggregation and review of more than two thousand references and were calculated under some basic assumptions (e.g. contributions from land-use change and heat production – as in the case of cogeneration – are not taken into consideration). The emissions are expressed in terms of grams of CO_2 equivalent emitted for unit of electricity produced (kWh), with a minimum and maximum peak due to different methods of evaluation in the reviewed literature reports and studies. In order to compare traditional fossil fuel sources and renewables energy it is necessary to base the calculation on a lifecycle approach; indeed normalizing the emissions generated by the specific technology in the entire life cycle (manufacturing, transportation, operation and decommissioning) with the electricity generated. As it is clearly visible, the main and most important result is that renewable energy technologies for electricity generation have lifecycle GHG emissions 20-50 times less than conventional fossil-based energy sources; and in this sense they can be considered clean, carbon-free energy resources.
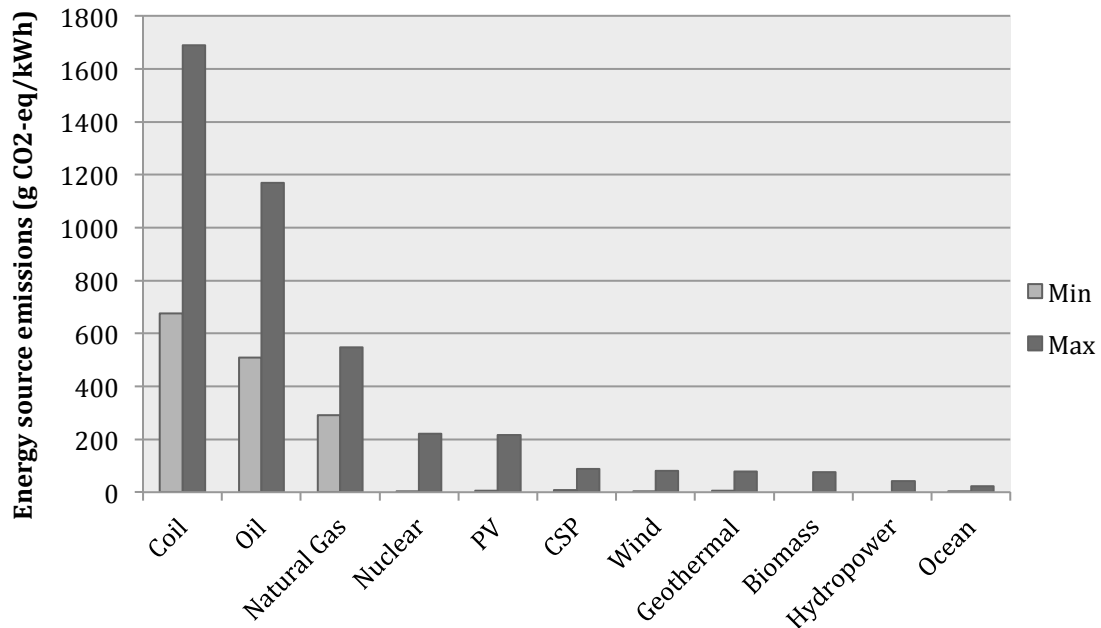
Figure 10. GHG emissions in grams of CO_2 equivalent per kWh of electricity produced for most diffused traditional and renewable energy sources. CSP=Concentrating Solar Power [8].

Natural gas (mainly methane) is largely used in developing and developed countries for electricity and power generation. The emissions associated with this source of energy are low (469 g CO2-eq/kWh in a 50th percentile distribution) compared to coal (1001 g CO2-eq/kWh) and oil (840 g CO2-eq/kWh) power plants, but they are still 30 times higher than emissions from nuclear power generation (16 g CO2-eq/kWh in a 50th

percentile distribution). Ultimately, for fossil-based fuels, natural gas and even for nuclear power generation, the factor of non-renewability must be taken into consideration: the increasing energy demand and the related rise in the extraction rate of these fuels are drastically decreasing their availability as nature reserves.

2.2   Carbon Capture

The last of the three pathways indicated as possible methods for GHG emissions reduction is carbon capture and subsequent sequestration (CCS) or utilization (CCU). According to a special report redacted by the IPCC, these technologies are considered as 'transitional technologies', with fast development from 2015 onwards and decay after reaching a peak in 2050 due to the gradual substitution of conventional fossil-based energy sources with carbon-free or carbon-reduced technologies [24]. Carbon capture will potentially account for up to half of the total GHG mitigation effort by the end of this century, indeed making it a significant tool for stabilizing atmospheric GHG concentration.

Carbon capture consists of the separation of CO_2 from gas mixtures mainly coming from exhausts of industrial or power plants. This technology can even be used for direct atmospheric CO_2 capture, or alternatively, CO_2 capture from the exhausts of power and industrial plants. The latter shows much higher efficiency than the former,

since the concentration of CO_2 in the air (0.04 mol%) is much less than the average concentration of CO_2 from the exhaust of power generation plants (12 mol%) [25]. For example, considering a 3,300 MW power plant (such as Monroe Power Plant in Michigan, USA) it is theoretically possible to capture 18.6 millions of tons of CO_2 per year [26]. Capturing the same amount of CO_2 directly from the air, assuming a 1 m/s flow rate, would necessitate a surface area of approximately 830,000 m^2.

The main separation technologies for carbon capture are absorption, adsorption, and membranes-based separation. They differ for capture efficiency, materials utilized and costs. In the absorption process, CO_2 is initially transferred from a gas phase to a liquid phase (through a solvent), and it is subsequently transferred back to the gas phase during the stripping process that is usually coupled to the absorption process. Solubility of CO_2 in the solvent, diffusion, and reaction kinetics are parameters that affect the overall capture rate together with the design parameters of the column in which the reaction occurs.

Differently, in the adsorption technology the gas mixture from the exhaust comes in contact with a sorbent in the form of small porous particles that adsorb or form a complex with CO_2. Activated carbon, zeolites, silica gel, activated alumina, ion exchange resins, hollow fibers, and chemisorbents are examples of traditional commercial sorbents for CO_2 adsorption. The capture is completed with a regenerative process, in which the final product is desorbed and the sorbent is regenerated for cyclic use.

The two capture processes detailed so far require phase changes (from gas to liquid or vice versa) and their integration in a power plant is not simple and can bring losses in efficiency. Membrane separation technologies, instead, can be easily integrated in existing emitting plants and they don't require regeneration processes and phase changes. On the other hand, they need a higher driving force; and therefore their utilization in traditional coal-fired power plants, with relatively low-concentration of CO_2 in the exhaust gas, is still challenging.

The integration of these technologies on new or existing emitting plants has a very high potential. IPCC estimates that emissions of a single plant that uses a carbon capture technology can be reduced up to 90% [24]. It is clear that this technology rationalizes the costs for its adoption and application. These costs mainly include the equipment cost (chemical used, reactors, etc.) and the cost of the power required to run the capture system. CO_2 concentration in the exhaust gas also affects the cost, since it influences the minimum work required for separation as dictated by thermodynamic laws. For example, in a plant emitting gas with a CO_2 concentration of 12 mol%, the estimated cost for carbon capture is 0.045 $/kg, compared to 0.059 $/kg of CO_2 captured in natural gas power plants (CO_2 concentration 3.7 mol%) or 1 $/kg cost estimated per direct-air capture (CO_2 concentration 0.039 mol%) [27,28,29]. In any case, the initial investment is the main obstacle to overcome for a wider distribution of this technology.
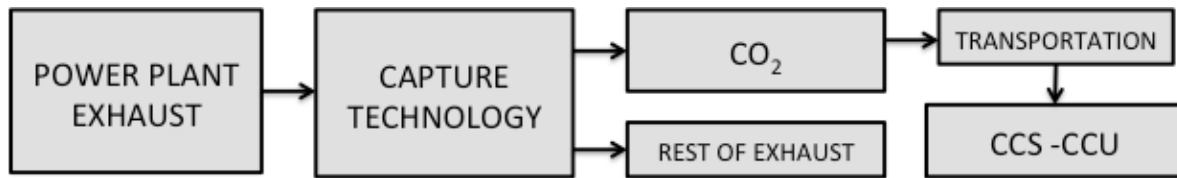
Figure 11. Schematic of carbon capture application.

There are other two methods for carbon capture from power generation that will not be discussed in detail. In the first (pre-combustion), the fuel utilized in the plant is pre-heated and converted into a mix of CO_2 and hydrogen before the combustion. CO_2 is then captured and hydrogen is used as fuel to produce electricity. In the second (oxy-fuel combustion), oxygen, and not air, is used to burn the fuel. The steam produced by the combustion allows an easy removal of CO_2, compared to traditional gas-mixtures.

In any case, once the CO_2 is captured, it must be compressed for transport. In order to avoid gas pressure drops, CO_2 it is compressed and cooled down to its liquid phase, and it is later transported through pipeline or ship transportation methods. This happens whether the CO_2 is subsequently stored (CCS) or it is utilized (CCU).

2.2.1 Carbon sequestration

Storage (sometimes referred to as sequestration) of CO_2 can be described simply as the injection of captured CO_2 into deep geological formations (such as porous rocks),

for a long-term storage. The first example of a commercial CSS plant was seen in 2000: everyday tons of carbon dioxide has been transported from a coal gasification plant in North Dakota to Weyburn, Canada through a pipeline connection where it is injected into Canadian soil. Although during the last decade a few other sites worldwide, varying from small pilots to large-scale plants, have been adopting this technology, CCS is still considered an under development technology that is facing the research and demonstration phase.

In the last two decades, another method of storage has been studied and considered. It consists of the dissolving of captured CO_2 in seawater. Unfortunately, experiments have shown that this method can be harmful for marine life at the point of injection; and in a long-term scenario ocean mixing can eventually release CO_2 back to the atmosphere. In conclusion, some recent studies have shown the high potential of the adoption of CCS technologies, with an estimation of nearly a 20% cut in global emissions by 2050 [30].

2.2.2 Carbon utilization

As previously mentioned, the captured carbon dioxide can be also subsequently utilized (CCU). There are mainly two pathways of utilization for CO_2. In the first one CO_2 is not converted into other chemical forms, and it is directly used as solvent (e.g. in

processing chemicals) or as a working fluid in various geothermal applications. Enhanced Oil Recovery (EOR) can be considered an efficient method of utilization for non-converted carbon dioxide: it has been estimated that 89 billion barrels of oil in the US alone could be recovered using the latest technologies for CO_2-EOR, at the same time storing large amount of carbon underground [31].

The second pathway for CO_2 utilization includes biomass generation, and chemical and electrochemical conversion to other energy storage chemical forms. Algal pond systems for CO_2 conversion to biomass represent the most economic methods to produce biomass on a large scale [32,33]. In an algal mass culture pond system using different types of CO_2 supply methods (such us bubbling or floating gas exchanger) at different volume concentrations, it is possible to obtain very high value products, mainly pharmaceutical or food grade products. Carbon is the dominant nutrient also in the case of biomass and biofuels production through photosynthesis microalgae bioreactors.

The potential of carbon dioxide conversion is substantial. In addition to biomass generation, CO_2 can be used for production of fuels and chemicals such as syngas, formic acid, methane, ethylene, methanol and dimethyl ether. Although there are no cases of commercialized processes for CO_2 conversion yet, the interest on this topic has been increasing during recent decades. A range of scientific and research areas have become involved, due to a higher shared awareness of problems related to GHG atmospheric concentration and global warming.

CHAPTER 3

ELECTROCHEMICAL REDUCTION OF CO2

Electrochemical reduction of CO_2 has been investigated extensively and it has been a candidate for a valid and efficient method of CO_2-to-fuel conversion. The energy required for the reaction can be provided either directly from solar light (photoelectrochemistry) or indirectly from electricity produced by any kind of renewable source. Although photoelectrochemical CO_2 reduction is becoming an increasingly attractive option thanks to the potential high efficiency of the process (no need of conversion of solar light to electricity), this technology presents non negligible limitations (e.g. need of semiconductor electrode) and its development is still challenging.

During last 20 years extensive research on photo- and electro-chemical CO_2 conversion has yielded large improvements on selectivity, cost, and efficiency of catalysts utilized. Several reviews have been redacted for electrochemical reduction of carbon dioxide and the technology seems to be mature, even if the effort is still at the laboratory scale [34,35,36,37]. The technology can be applied in a compact system, at room temperature and ambient pressure, with the possibility to scale up fairly easily. Moreover, the process can be driven by renewable source of energy (solar, wind, geothermal, hydroelectric, etc.), therefore operating as a renewable energy storage

mechanism. Solar light energy and solar thermal energy can also enhance the conversion, reducing the amount of external energy actually needed for the reaction (i.e. photoelectrochemistry). The desired reaction products are an easily transportable medium for energy storage in the form of alcohols and fuels (HCOOH, CO, methanol, ethylene, methane) with attractive high recoverable energy density (compared to, for example, Li-ion batteries, traditional batteries or flywheels) [38].

Despite the listed positive aspects, the DOE identifies the major obstacle for an efficient and effective CO_2 conversion by electrochemical reduction as the lack of a catalyst capable of achieving selective break of C-O bonds in carbon dioxide, using Earth abundant sources of energy, and low-cost reducing agents [39]. An optimum catalyst would show high energy efficiency (low overpotential), high current density (high rate of reaction), high faradaic efficiency (F.E.) for the desired product (catalytic selectivity), and a long lifespan.

3.1   Thermodynamic and kinetic considerations on CO_2 reduction

Carbon dioxide is a thermodynamically and kinetically stable molecule. Its reduction favors multi-electron steps with proton coupling (Equations 3.1-3.5), since more thermodynamically stable molecules are obtained.

$$CO_2 + 2H^+ + 2e^- \rightarrow CO + H_2O \qquad\qquad E^0 = -0.53\,V \qquad\qquad (3.1)^a$$

$$CO_2 + 2H^+ + 2e^- \rightarrow HCO_2H \qquad\qquad E^0 = -0.61\,V \qquad\qquad (3.2)^a$$

$$CO_2 + 4H^+ + 4e^- \rightarrow HCHO + H_2O \qquad\qquad E^0 = -0.48\,V \qquad\qquad (3.3)^a$$

$$CO_2 + 6H^+ + 6e^- \rightarrow CH_3OH + H_2O \qquad\qquad E^0 = -0.38\,V \qquad\qquad (3.4)^a$$

$$CO_2 + 8H^+ + 8e^- \rightarrow CH_4 + 2H_2O \qquad\qquad E^0 = -0.24\,V \qquad\qquad (3.5)^a$$

$$CO_2 + e^- \rightarrow CO_2^{*-} \qquad\qquad E^0 = -1.90\,V \qquad\qquad (3.6)^a$$
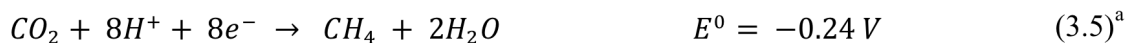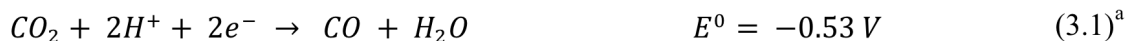
[a] potential versus NHE at pH 7 in aqueous solution, 25°C, 1 atmosphere gas pressure, and 1M for the other solutes [36].

However, in the kinetics of the reaction the actual potentials are much higher than the thermodynamic potentials showed in Equations 3.1-3.5, since the reaction involves the formation of intermediate complexes that occurs at much higher potentials. In 1969, Paik *et al*. were the first to propose that the reaction for CO_2 conversion is preceded by the formation of an intermediate complex (CO_2^{*-}) [40]. Later works confirmed the formation of the complex; and by the use of spectroscopic techniques, it was shown that the formation of the one-electron reduction intermediate is responsible for the low reaction rate as well as the high over-potential required for the reaction (Equation 3.6) [41].

Benson *et al*. identifies two main pathways in which CO_2 chemical bonds can be broken to promote the formation of more complex and energetic molecules [42]. The first

approach is the conversion of CO_2 into a mixture of CO and H_2 (also called syngas or synthesis gas), which in a subsequent step can be used directly as a fuel for a syngas engine, or utilized as an intermediate for production of ammonia and methanol, or converted to liquid fuels through the Fischer-Tropsch process. The electrochemical reduction of CO_2 into CO and H_2 involved in the first pathway is the 'easiest' conversion from a thermodynamic and kinetic perspective: the Nerst potential for formation of CO is the lowest (see Equation 3.1) and the reaction involves 'only' two electrons. Moreover the electrochemical conversion is hydrogen-proton coupled and in most cases H_2 formation occurs as a concurrent reaction. The second pathway is more challenging from the kinetic point of view, and it implies the direct formation of liquid fuels through the electrolysis process. In this case, four- six- and eight-electrons charge transfer is required for the formation of the desired products.

However, in both the paths described, the functionality of the catalyst and the medium for the reaction is of main importance. The distribution of the products (catalytic selectivity) and the efficiency of the reaction (current efficiency and overall energy efficiency) strongly depend on the selection of the catalyst and the medium.

3.2   **Classification of catalytic systems for electrochemical reduction of CO_2**

Electrochemical reduction of CO_2 systems can be subdivided into two main categories: systems that perform the reaction in an aqueous medium, and systems that use a non-aqueous medium. Different catalytic systems belong to both or one of the two categories. It is possible to distinguish among heterogeneous catalytic systems, which mainly operate through bulk metal cathodes, and homogeneous catalytic systems, which perform the reaction through transition-metal complex-based catalytic systems [43].

3.2.1   **Heterogeneous electroreduction of CO_2 in aqueous medium**

There is an enormous amount of data reported for CO_2 reduction, and most of the classifications adopted rely on the nature of the main products. In an aqueous solution, different metal electrodes for heterogeneous electrochemical CO_2 reduction can produce:

- Hydrocarbons and alcohols (Cu)
- Formic acid (In, Sn, Hg, Pb)
- Carbon monoxide (Zn, Au, Ag, Pd, Ga)
- Other products (in insignificant quantities)

As previously mentioned, in aqueous medium, hydrogen evolution reaction (HER) occurs as concurrent reaction competing with CO_2 reduction. As revealed by Hori

and Suzuki, given a fixed potential, HER rate is proportional to the pH (proton activity) of the electrolyte and indeed is prevalent in acidic solutions [44]. At higher overvoltage, hydrogen evolution is usually, but not always, suppressed and the formation of the desired product (CO, HCOOH, CH$_4$, etc.) is favored.

Hydrocarbons and alcohol formation at Cu electrodes has been extensively studied and reported in last 20 years [45,46,47], and there are excellent reviews on the literature [48,49,50]. In the kinetics of the reaction CO plays an important role, since it is the intermediate product for the formation of hydrocarbons (mainly ethylene and methane). After applying a certain overpotential, carbon monoxide begin to be reduced and accumulated at the electrode. At this point the hydrogen evolution is suppressed and the formation of hydrocarbons is promoted (with ethylene formation favored over methane at lower overpotentials [51]). Faradaic efficiencies of ~70% for the production of hydrocarbons have been reported in potassium bicarbonate solution (0.1 M KHCO$_3$) and at reasonable reaction rates (up to 7 mA/cm^2 current density) [35]. However, the multi-step characteristic of the reaction kinetics implies that high negative potentials (low energy efficiency) are required for the reduction (-1.4 V vs. SHE) [35]. Although copper shows excellent catalytic selectivity and high current efficiency, the high energy required for the reaction eliminates copper as an ideal catalyst for CO$_2$ reduction.

Eyring in 1969 led the first group that detected formic acid production at high current efficiency (>50%) occurring at the mercury electrode in acidic and neutral

solutions. They reported faradaic efficiency close to 100% for the formation of HCOOH in a lithium bicarbonate solution, but at low current density (~0.3 mA/cm^2) [40]. They also proposed a possible mechanism for the kinetics of the reaction. Several works have been later reported on CO_2 electroreduction to formic acid on Hg, Pb, In, and Sn solid electrodes [52,53,40]. High-pressure and high-temperature catalytic systems have been found to enhance the efficiency of the conversion and have been largely used for formic acid production. Köleli and Balun recently investigated electrochemical reduction of CO_2 in a fixed-bed reactor using Pb-granules electrodes and 0.2 M K_2CO_3 as an electrolyte [54]. Current efficiency for formic acid formation was high (94%) but at the expense of a negative cathode potential (-1.56 V vs. SHE). Current density was still low at standard environmental conditions (~0.6 mA/cm^2) but they showed how it is possible to enhance the reaction rate by increasing temperature and pressure in the reactor, maintaining high current efficiency. Hori *et al*. reported higher current efficiency (97.5%) at higher current density (5 mA/cm^2), running an experiment at room temperature in 0.1 M $KHCO_3$. However, the energy required for the reaction was still too high (cathode potential of -1.63 vs. SHE) for any attractive efficient application [55]. Interestingly, in 2012 Zhao and co-workers investigated for the first time the electroreduction of CO_2 utilizing environmentally friendly microbial fuel cells (MFC). Connecting several MFCs in series, they increased the input voltage of the overall system, making it comply with the CO_2 reduction voltage requirement. The carbonaceous substances (mainly organic sludge from wastes and wastewaters plants) utilized for the reaction transform chemical energy

into electrical energy that is in turn used in-situ to reduce the CO_2 emitted from the degradation process to formic acid. Impressively, a faradaic efficiency of 64.8% for the formation of HCOOH was achieved. The absence of an external energy supply requirement and the high current efficiency make the system attractive for further studies and development.

Ultimately, Zn, Au, Ag, Pd, Ga, are selective metal catalysts for CO formation by electrochemical reduction of CO_2. The thermodynamics and kinetics of the reaction suggest that CO is the easiest molecule that can be obtained by CO_2 reduction (Equations 3.1-3.5), and in fact, its formation has been reported to occur at the lowest overpotential. In 1994, Hori *et al*. showed that the energy barrier for the formation of the desired product is significantly reduced in the case of Au and Ag metal electrodes, with high selectivity for CO formation (up to 87%) [55]. The experiments, carried out maintaining same electrolyte (0.1 M $KHCO_3$) and same current density (5 mA/cm^2) for different metal electrodes, indicated a cathode potential of -1.14 V vs. SHE in case of gold electrodes, and -1.37 V vs. SHE in case of silver electrode. Whereas on one hand, the work redacted by Hori *et al*. has noted the interesting properties of these noble metals compared to other catalytic systems for CO_2 reduction, on the other hand, several other studies have been carried out with the aim of developing Au- or Ag-based catalyst for high energy efficiency CO_2 reduction [56,57,58]. The reaction at Au and Ag electrodes not only occurs at low overpotential, but it is usually associated with high current

density, high current efficiency, and relatively high stability of the catalyst in time. Drawbacks of the use of these metals (valid in general for all metal electrodes) are: the high costs (especially for noble metals); the suffering of corrosion; and the problems related to deactivation or passivation of the catalyst in long-term electrolysis. CO formation at gold electrodes in an aqueous medium begins at -0.8 V vs. SHE and it does not depend on the pH of the electrolyte, since the proton donor is not H^+ but H_2O molecules [59]. CO_2 conversion properties on Ag electrodes have been demonstrated to depend on crystal orientation at the metal surface, and nanoparticles size (in the case of a metal nanoparticles catalyst) [60,61]. A recent work reports almost negligible overpotential for CO_2 reduction to CO, at almost 100% current efficiency and reasonably high current density. It will be discussed in detail below.

3.2.2   <u>Non-aqueous mediums for electrochemical CO_2 reduction</u>

Non-aqueous solutions for CO_2 reduction have also been largely used thanks to some important properties they show. Primarily, the absence of water prevents hydrogen evolution. Secondly, CO_2 in organic solvents can be dissolved in much higher concentration than in water solutions. Mainly metal electrodes have been adopted for CO_2 reduction in non-aqueous medium and methanol is abundantly used as solvent.

Depending on the operating conditions, the catalysts, and the electrolyte used, it is possible to obtain CO, HCOOH, and $(COOH)_2$ at quite high current efficiencies [62].

3.3   Electroreduction of CO_2 to CO at Ag electrodes in EMIM-BF$_4$ ionic liquid

3.3.1   Ionic liquids

Academic and industrial interest on ionic liquids has been growing exponentially in the last 20 years. They are widely used across many applications: as powerful solvents, as thermal fluid for heat storage, and as electrolytes. Some modern ionic liquids have attractive properties for electrolysis applications, compared to traditional ionic liquids and other ordinary liquids (such as acids or water solutions). Low vapor pressure, high ionic conductivity (in the range of aqueous electrolytes values), and the ability to behave as a catalyst make new ionic liquids suitable solvents for electrochemistry, in contrast with volatile organic solvents and their inherent environmental-related problems [63,64,65].

3.3.2   EMIM-BF$_4$ electrolyte for CO_2 reduction

Different ionic liquids have been investigated for electrochemical CO_2 reduction with remarkable results [66,67]. In a recent work, the use of an aqueous solution of 1-

ethyl-3-methylimidazolium tetrafluoroborate (EMIM-BF$_4$ – chemical structure is shown in Figure 12) ionic liquid in a flow reactor has been demonstrated to enhance the electrocatalytic properties for CO$_2$ conversion, reducing the energy barrier for the formation of CO. The high selectivity for carbon monoxide production was given by the utilization of silver as the working electrode (cathode).
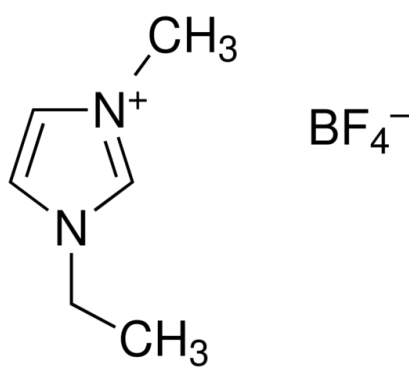
Figure 12. Chemical structure of 1-ethyl-3-methylimidazolium tetrafluoroborate

(EMIM-BF$_4$) ionic liquid

Interestingly, not only was a negligible overpotential for the reaction (0.17 V) observed, but also high current efficiency and quite high robustness of the system over time, with over 96 % F.E. reported in a 7 hour-long experiment. It was proposed that the use of this specific ionic liquid would facilitate the formation of a complex between the cation of the electrolyte (EMIM$^+$) and the CO2^{*-} intermediate. The formation of the complex (EMIM$^+$–CO2^{*-}) would occur at low cathode potential (-0.25 V vs. SHE)

thereby drastically reducing the energy barrier for CO_2 reduction, as shown in Figure 13 [68].
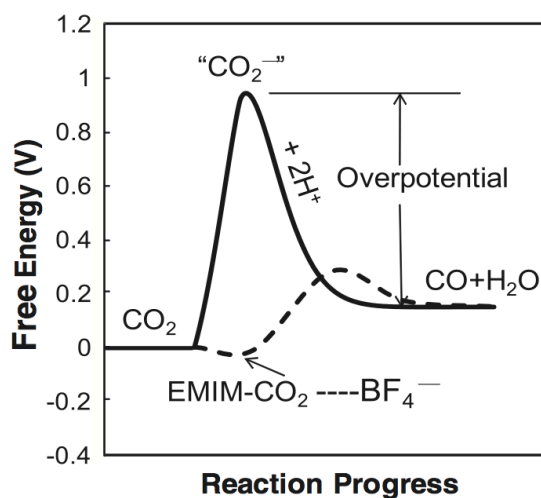
Figure 13. Schematic of free energy path for formation of CO in water or CH_3CN (solid line) and in EMIM-BF_4 (dashed line).

The use of this co-catalyst system (EMIM-BF_4 electrolyte + Ag cathode) can be considered a breakthrough in the CO_2-to-fuel conversion via electrochemical reduction. Energy efficiencies of up to 87% percent for CO production have been reported, making this electrocatalytic system a suitable candidate for possible scale-up applications. Unfortunately there are other issues that hinder large-scale development. First, is the high-cost associated with the necessary noble metal (Ag) as an electrode. Second, is the low observed turnover rate (~1 s^{-1}), which is one order of magnitude less than what is required for a commercial process.

In next chapter, an ionic liquid-mediated system for production of syngas (CO + H_2) by CO_2 electrochemical reduction is presented. The utilization of a low-cost transition metal catalyst, and the high current density reported, potentially overcome the weaknesses reported by previous works, making this new catalyst system a strong candidate for industrial applications of the CO_2-to-fuel conversion.

CHAPTER 4

SOLAR ENERGY DRIVEN MICROFLUIDIC REACTOR

The intermittent nature of renewable energies (solar, wind, etc.) and the difficulties associated with their integration in the existing electricity grid stress the necessity of a flexible method to store the available energy in a portable form. Storing the excess energy produced by renewable sources into chemical forms (such as fuel) would represent a favorable method to address the issues related to the adoption and development of renewable energy technologies. The synthesized chemicals and fuels can be later transported and utilized, making energy available when, and where, renewable technologies are not able to produce it (e.g. during the night in the case of photovoltaic plants).

Recently, the prospect of hydrogen being an efficient energy vector has motivated several works and studies on this subject. Industrialization and commercialization cases of 'clean' hydrogen-based fuel processes, such as water electrolysis for hydrogen production and fuel cells for electricity generation by hydrogen, have been increasing in the last decade, supported by strong policies and incentives mainly in developed countries. Unfortunately the development of this technology faces two main obstacles: low energy density of the hydrogen itself, and the necessity of modifications to the existing infrastructures for transport and utilization.

Synthesis of hydrocarbon-based fuels from CO_2 (i.e. captured CO_2) would result in higher energy density vectors (up to 15 times more than hydrogen) [69] that are also compatible with the existing infrastructures. Moreover, the process not only could use renewable resources for the energy required for the conversion (taking part in the carbon energy cycle shown in Figure 13), but would also contribute significantly to the reduction of CO_2 emissions.
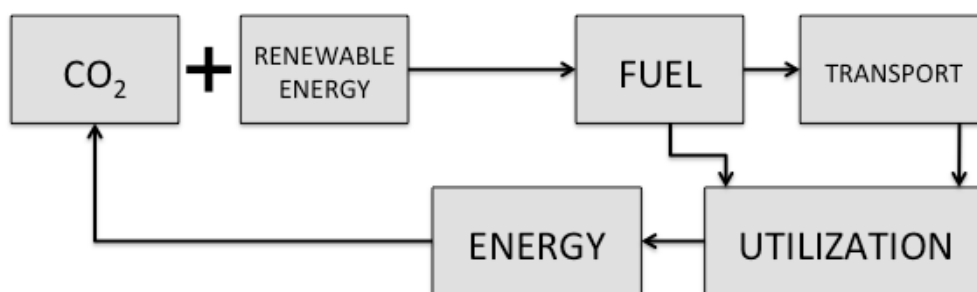
Figure 14. Schematic of a potential carbon energy cycle for CO_2-to-fuel conversion technology application.

As it has been discussed in Chapter 3, electrochemical reduction of CO_2 is the strongest candidate to perform the CO_2-to-fuel conversion at attractive energy efficiencies for industrialization. A co-catalyst system was recently discovered showing high faradaic efficiency for CO formation and almost negligible overpotential. Low current density (low turnover number) and the utilization of a high-cost noble metal (Ag)

electrode represent the weaknesses of this discovered system. This chapter will present a new low-cost co-catalyst system able to perform electroreduction of CO_2 at a much higher current density than previously reported, using a transition-metal catalyst and an electrolyte in 96 mol% of water solution. The system boasts selectivity for CO formation of up to 97.5 %. It is also observed that the applied potential affects the CO/H_2 ratio production, representing a potentially adjustable system for syngas production. The energy required for the reaction is provided directly by a 6-Watt solar panel. The output voltage of the photovoltaic unit is reduced by a DC/DC regulator and then applied to the reactor. In this configuration, there is no need for a DC/AC power inverter unit, which allows for a considerable cut in the overall costs.

4.1 Molybdenum disulfide catalyst for electrochemical CO_2 reduction in EMIM-BF_4 aqueous solution

Molybdenum disulfide (MoS_2) is an inorganic compound belonging to the transition-metal sulfides group. Scientific interest in this material has been increasing recently thanks to its attractive chemical and physical properties. It is commonly used in different technological sectors, mainly in lubrication, electronics, and for catalysis applications (e.g. hydrodesulfurization in petroleum refining).

Recent works demonstrated remarkable properties of nanostructured MoS_2 for photo- and electro-chemical water splitting, making it an inexpensive substitute for

platinum in hydrogen production from water electrolysis [70]. The prominent results of the catalytic activity of MoS_2 for electrochemical conversion of CO_2 into syngas are reported in this paper.

In order to investigate the electrocatalytic properties of MoS_2 for CO_2 reduction, cyclic voltammetry (CV) and chronoamperometry (CA) were performed in a standard three-electrode electrochemical cell (see Methods and Materials). Impressively, the bulk MoS_2 catalyst showed 60 times higher current density than a bulk Ag catalyst at a cathode potential of -1.0 V vs. SHE [68]. Moreover, the experiments were carried out in a less concentrated (and therefore lower cost and more environmentally-friendly) ionic liquid solution in water (4 mol% EMIM-BF$_4$, 96 mol% H_2O), compared to solutions previously reported. To emphasize the importance of the results, Table I presents a comparison between MoS_2 and Ag catalysts according to the experimental results of both this paper and previous publications. It is also interesting to notice that the Ag bulk catalyst shows almost 0 % catalytic selectivity for CO production in the low concentrated 4 mol% solution, indicating that the entire current efficiency is utilized for hydrogen evolution. On the other hand, if silver nanoparticles (Ag NPs) are used rather than bulk silver, the current efficiency for CO formation shifts from ~ 0 % up to ~ 80 % [71].

TABLE I. COMPARISON OF CATALYSTS FOR CO_2 REDUCTION IN EMIM-BF_4

SOLUTIONS AT -1.0 V vs. SHE

Catalyst	Current Density (mA/cm^2)	Electrolyte	CO F.E.	Reference
MoS_2 Bulk	60	4 mol% EMIM-BF_4	97.5 %	[d]
Ag NPs (<50nm)	7	4 mol% EMIM-BF_4	~ 80 %	[71]
Ag Bulk	3	4 mol% EMIM-BF_4	~ 0 %	[d]
Ag Bulk	1	18 mol% EMIM-BF_4	96-98 %	[68]
Ag NPs (5nm)	0.8 [b]	75ppm water[c]	96-98 %	[61]

[b] max. current density -1.2 mA/cm^2 at -0.75 V vs. SHE
[c] at higher water concentration would show higher current density
[d] experimental work for this paper

Other relevant results emerged from the electrochemical cell experiments. Firstly, the onset potential for CO formation was observed to occur at -0.5 V vs. SHE, just 0.17 V higher than the thermodynamic potential for CO formation in a solution of pH 4 (-0.339 V vs. SHE). Secondly, it was observed that production of CO/H_2 increases/decreases when the potential is switched from -0.5 V to -1.0 V vs. SHE.

In the context of electrochemical CO_2 reduction, hydrogen is often considered an "undesired product." The main reason is that if hydrogen evolution is present, part of the energy needed for the reaction it is "wasted" for the formation of H_2 molecules. However, the system here reported the presence of a singular property associated to the concurrent production of hydrogen during the reaction. The ratio between CO and H_2

formation is evidently "tunable," and it varies based on the cathode potential applied to the system (Figure 15). At the same time no other products were detected (or were present in less than 3 ppm, the detection limit of the GC) for all the time of the reaction, resulting in a clean process from this point of view. This promising result could represent an enormous advantage in the prospect of an industrialized process for the conversion of captured CO_2 into fuel (syngas in this case). The CO/H_2 ratio production can be adjusted according to the syngas required for any given application (i.e. for Fischer-Tropsch Synthesis the CO/H_2 composition ratio of syngas can vary between 0.5 and 1 depending on the catalyst utilized).
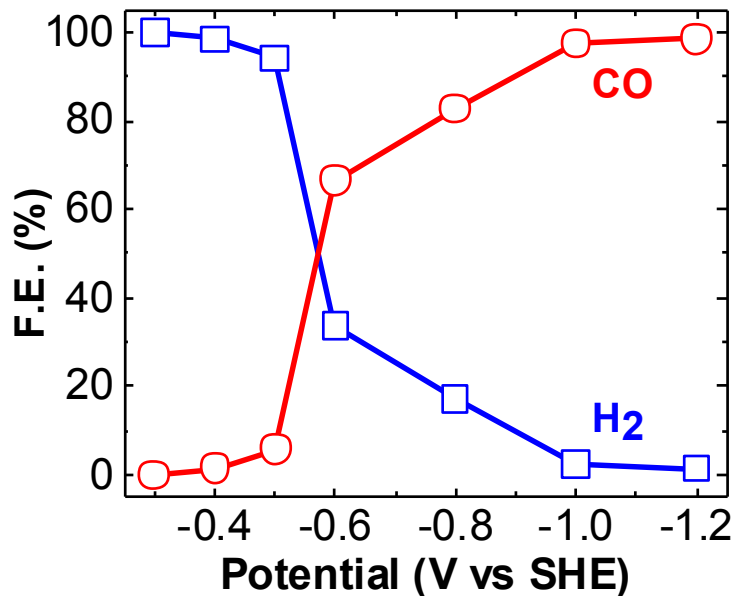

Figure 15. CO and H_2 faradaic efficiency trends plotted as functions of the potential applied at the bulk MoS_2 cathode. (See Method and materials for further information).

4.2   Solar energy driven microfluidic reactor

Once the electrochemical activity of the new catalyst had been tested in an electrochemical cell (batch process) showing impressive and promising results for the utilization of MoS_2 in electrochemical conversion of CO_2 to syngas, the co-catalyst system (MoS_2 + EMIM-BF_4/H_2O) was subsequently adapted and integrated in a microfluidic reactor for continuous CO_2 reduction. A potentiostat was first used to analyze the electrochemical behavior of the reactor. A solar panel was ultimately utilized to provide the DC voltage required by the reaction.

4.2.1   Reactor design

Various reactor designs have been recently proposed for electrochemical CO_2 reduction and most of these are based on pre-existing fuel cell designs. The reactors reported so far in this context have been mainly utilized for continuous production of formic acid and carbon monoxide [72,73]. There are essentially two different approaches for the design of reactors for electrolysis of CO_2. One uses a polymer electrolyte, as in most fuel cell designs. In another, instead, it is a liquid electrolyte that separates the cathode from the anode, and it is for this reason that it is classified as microfluidic reactor. The reactor designed, manufactured, and utilized in this work is of the 'microfluidic' type and its exploded view is shown in Figure 16. The reactor is characterized by a co-current flow of gaseous CO_2 and liquid catholyte on the cathode

part (top) and a flow of liquid anolyte in the same direction on the anode part (bottom). An ion-exchange membrane is placed between the two liquids, which separates the catholyte from the anolyte maintaining electrical conductivity. Gas diffusion electrodes (GDEs) are used as the cathode and anode. The catalyst (MoS_2 for the cathode, and Pt for the anode) is applied on the side of the GDEs that face their respective liquid (see Methods and materials). The use of a separated catholyte flow on the anode part is suggested by the fact the Pt catalyst would otherwise be poisoned and therefore deactivated by the CO produced at the cathode [68]. The CO_2 flows from a gas channel that also operates as the cathode current collector. CO_2 then diffuses through the GDE, mixing with the catholyte ($EMIM\text{-}BF_4$ + H_2O) and reacts at the catalyst surface producing CO. Schematics of the half-reactions that occur at the electrodes are shown on Figure 17 and Figure 18.

Although, this design (GDEs + catholyte flow + membrane + anolyte flow) has its detriments, including an increasing resistance across the membrane during long-term experiments, this microfluidic configuration presents several advantages in terms of flexibility in operating conditions (e.g. the ability to easily change the electrolyte composition) and in terms of minimization of water management issues at the electrodes.
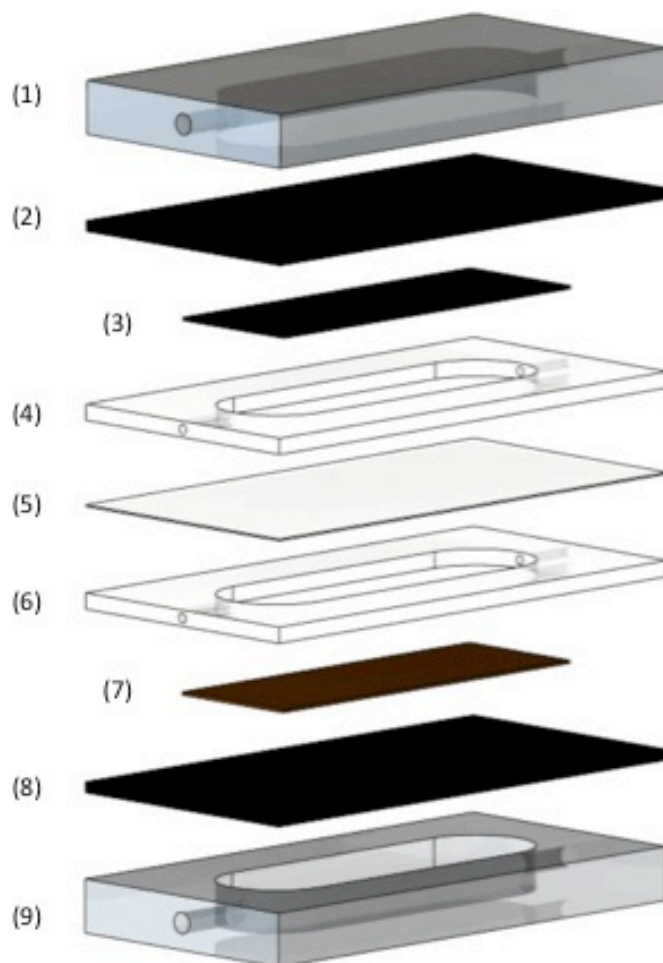
Figure 16. Exploded view of the microfluidic reactor for electrochemical CO_2 reduction. (1) Cathode current collector/Gas channel for CO_2; (2) GDE cathode; (3) MoS_2 catalyst; (4) Teflon liquid channel for catholyte; (5) Membrane; (6) Teflon liquid channel for anolyte; (7) Pt catalyst; (8) GDE anode; (9) Anode current collector/Gas channel for O_2.

4.2.2 <u>Reactor operation</u>

The reactions occurring in the reactor (as in most of the reactors of this type) are reduction-oxidation (redox) reactions. In general, in the oxidation step (at the anode) electrons are released due to the oxidation of a chemical species. The electrons are sent to an external load and, through it, flow toward the cathode. At the cathode a chemical species is reduced, acquiring the electrons coming from the eternal load. The full redox reaction can be therefore divided into two half-cell references that develop in physically separate regions of the reactor. The electrolyte interconnects the two regions (cathode and anode) providing the conductions of ions.

In order to give a clear schematic, the two half-cell reactions will be isolated and considered separately. The overall reduction reaction occurring at the cathode is shown on Figure 17. However, as proposed by Rosen *et al.*, the conversion of CO_2 to CO occurs thanks to intermediate reactions involving the formation of a complex in the heterogeneous interaction between EMIM-BF_4 (liquid) and CO_2 (gas) (Equation 4.1) [68,74]. The complex later interacts with the hydrogen protons, provided by the oxidation that develops at the anode, producing gaseous CO and releasing the OH^- anion and $EMIM^+$ cation (Equation 4.2). Finally hydroxide and hydrogen protons react, producing water (Equation 4.3).

Figure 17. Schematic of the reactions occurring at the cathode of the microfluidic reactor. (Dimensions are exaggerated for clarity).

Equations 4.1-4.3 represent the three intermediate steps for the development of CO in the catholyte. Equation 4.4 represents the reduction reaction through which the hydrogen is produced in the system. Ultimately other minor reactions can occur at the cathode, and they are not reported due to the small impact they have on the overall reaction.

$$EMIM^+ (l) + CO_2 (g) + e^- \rightarrow complex^- (l) \tag{4.1}$$

$$H^+ (l) + complex^- (l) \rightarrow CO (g) + OH^- + EMIM^+ (l) \tag{4.2}$$

$$OH^- + H^+ (l) + e^- \rightarrow H_2O (l) \tag{4.3}$$

$$2H^+ + 2e^- \rightarrow H_2 \qquad\qquad (4.4)$$

On the anode side of the cell the kinetic of the reactions is different. Platinum nanoparticles (utilized as catalyst) are in contact with a low-concentration solution of sulfuric acid; which, as previously mentioned, avoids the poisoning of the platinum catalyst by the CO produced at the cathode, and at the same time maintains the electrical conductivity through the cell. The main reaction occurring at the anode is the *water-splitting* reaction, in which water molecules are separated into hydrogen protons and oxygen while electrons are simultaneously released (Figure 18). The potential applied to the cell then drives hydrogen ions toward the cathode side where they participate either in CO_2 conversion to CO (Equations 4.1-4.3) or in H_2 production (Equation 4.4).
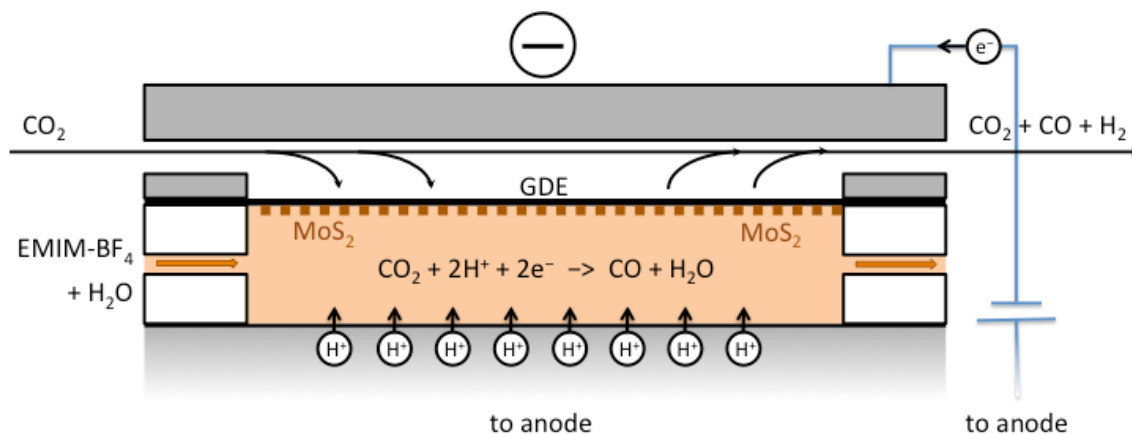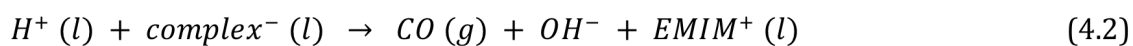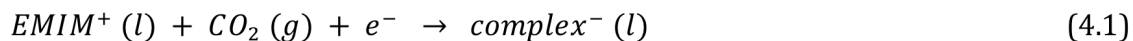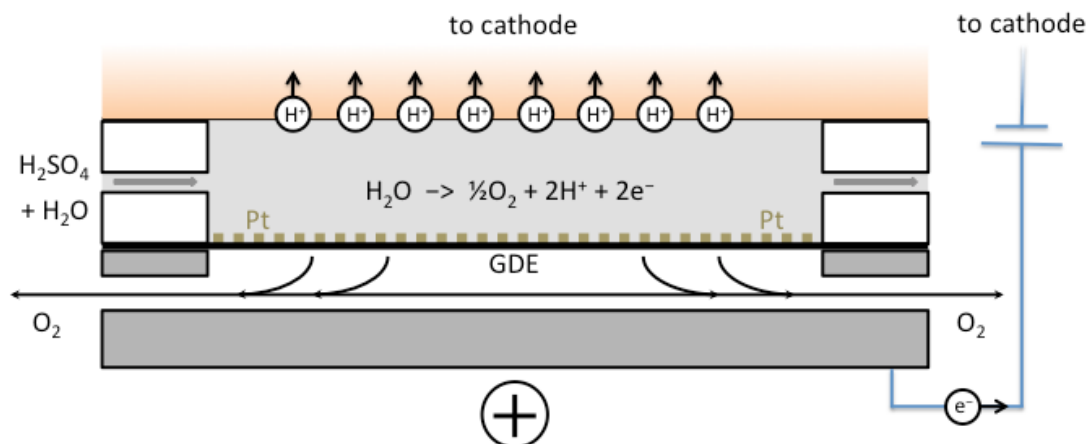

Figure 18. Schematic of the reactions occurring at the cathode of the microfluidic reactor. (Dimensions are exaggerated for clarity).

4.3   **Methods and materials**

4.3.1   **Methods and materials for three-electrode electrochemical cell**

The experiments to investigate the catalytic activity of MoS_2 were carried out in a three-electrode electrochemical cell. A schematic of the cell is shown in Figure 19. The working electrode (WE) was represented by a piece (5mm x 5mm) of a single crystal of MoS_2 (purchased through SPI Supplies). An aluminum crocodile clamp and a copper wire allowed for the electrical connection of the MoS_2 crystal to the exterior of the cell for electrochemical measurements. The counter electrode (CE) was a 25mm x 8mm platinum gauze 52 mesh (purchased via Alfa Aesar), which was connected electrically by a silver wire (0.5mm dia.). The reference electrode (RE) was a 0.5 mm dia. silver wire, annealed 99.9 % metal basis (purchased through Alfa Aesar). Counter and reference electrodes were washed several times in acetone and isopropanol and subsequently rinsed in DI water and dried with dry Nitrogen (AirGas) prior to use. No particular treatments were adopted for the working electrode. A water solution of 1-ethyl-3-methylimidazolium tetrafluoroborate (EMIM-BF$_4$, purchased through Sigma-Aldrich) was utilized as the electrolyte.

To characterize the MoS_2 catalyst for CO_2 reduction, the following procedure was adopted. Ultra High Purity Argon (AirGas) was initially bubbled for 2 hours into the cell through a mass flow controller and a 1/4 in. PVC tube was submerged into the solution at a particular ionic liquid concentration. With the same method, anaerobic CO_2 (AirGas)

was then sparged into the same solution at 1 sL/min flow rate and 40 psi until a saturated condition was reached (2 hours). The system was then ready for electrochemical measurement. A potentiostat (CH Instrument, model 600D) was utilized to obtain cyclic voltammetry (CV) curves, and the cathode potential was applied between 0 V and -1.8 V vs. silver wire. Maximum current density was obtained at a cathode potential of -1.8 V vs. silver wire (-1.0 V vs. SHE) with an electrolyte composition of 4 mol% EMIM-BF$_4$ and 96% mol% water. In order to analyze the catalytic selectivity of the system, the concentration of the electrolyte was kept constant (4 mol% ionic liquid) and chronoamperometry (CA) was run at different cathode potentials. The same procedure was adapted and the same potentiostat was used to obtain CA curves. Prior to running experiments, it was ensured that the cell was sealed and no leakages were present for gas to escape. CA was run in sequence at a cathode potential of -1.2 V, -1.4 V, -1.6 V, -1.8 V and -2.0 V vs. silver wire. For each experiment the potential was kept constant for 1 hour, after which a 2 mL gas sample was extracted with a plastic syringe from the cell and injected into the GC (SRI Gas Chromatograph, model 8610C) for gas detection. The results obtained are shown on Figure 20.
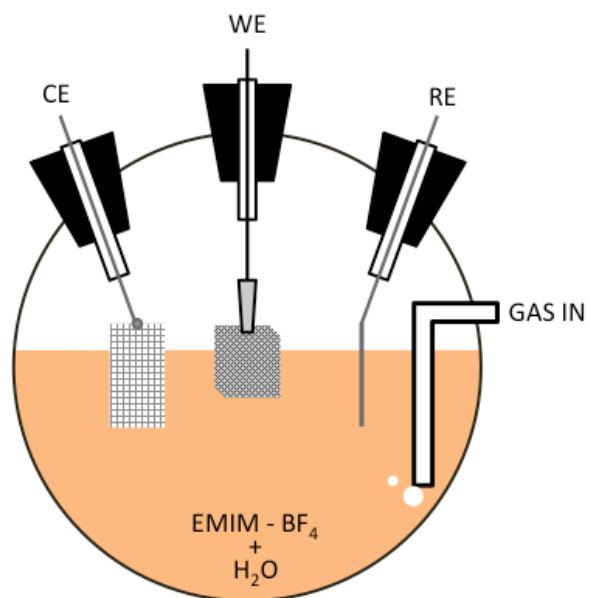
Figure 19. Schematic of the three-electrode electrochemical cell.

4.3.2   Methods and materials for microfluidic reactor

The reactor was initially connected to a potentiostat (CH Instrument, model 600D), for preliminary testing. In CA mode, short-circuiting the counter and reference connections of the potentiostat at the anode of the reactor made it possible to apply a cell potential (potential difference between cathode and anode) and to read the current at the same time. A silver wire connected downstream of the catholyte flow served as the reference electrode. Therefore, it was possible to monitor the cathode potential (potential difference between cathode and reference electrode) using a multi-meter. The cathode

and the anode were represented by GDEs which were painted with their respective catalyst. The cathode catalyst-ink was prepared by mixing 10 mg of MoS_2 nanoparticles (135 nm average dia., purchased through US Research Nanomaterials) in a solution of 0.6 mL isopropanol, 0.6 mL DI water, and 0.01 mL of 1100 EW 5% Nafion solution (DuPont). The ink was then sonicated for 5 minutes before being applied into an area of 2 cm^2 on the GDE using a paintbrush. The same procedure was adapted for the anode catalyst-ink, except that 10 mg of black platinum nanoparticles (5 nm, Alfa Aesar) were utilized in place of the MoS_2. The cathode and anode were in contact with their respective aluminum current collectors. These also served as gas channels to flow CO_2 into the reactor at the cathode, and to flow O_2 out from the reactor at the anode. Ten insulating nylon bolts held the setup together. A 4 mol% solution of EMIM-BF_4 in water operated as the catholyte, whereas a 0.1 M solution of H_2SO_4 was used as the anolyte. A syringe pump (Harvard Apparatus, model Elite11) facilitated the continuous flow of the liquids into the cell (at 0.25 mL/min flow rate) via two 8-inch stainless steel needles (0.9 mm dia. tip) connected at the inlet of the two Teflon liquid channels of the cell. The catholyte and anolyte were separated by a 3 cm^2 piece of Nafion-117 membrane, whose functionality has been previously discussed. A mass flow controller (Sierra Instrument, model SmartTrack 50) connected to the top gas channel through a 2 mm dia. stainless steel tube, was used to supply the CO_2 at 2.5 sccm flow rate. The gas channel exit was connected to the GC for gas detection through an external 3-port valve (provided by SRI), which is capable of injecting a 1 ml sample for detection. The column and the

thermal conductivity detector (TCD) of the GC were kept at 100 °C and 110 °C respectively and helium was utilized as carrier gas. The detection occurred 10-15 minutes after the cell potential had been applied in order to give time for the reactor to stabilize and to reach steady-state condition. After several CA experiments had been conducted by powering the cell through the potentiostat and after the products had been detected, the reactor was connected to a solar panel (Coleman, 6 W, 12 V) in order to prove that the reactor could be powered by a renewable source of energy. A DC/DC regulator permitted a step-down of the potential supplied by the PV unit to the value required by the cell. Ultimately a custom-made solar light simulator was utilized to provide the energy to the solar panel.

In Figure 20 it is shown a picture of the actual setup utilized for the experiments. Three main elements are easily recognizable in the picture: i) the mass flow controller (on the left) used to control the mass flow rate of the gaseous CO_2 injected into the cell, ii) the syringe pump that provides controlled liquid flow both for the ionic liquid solution (catholyte) and for the sulfuric acid (anolyte), iii) the reactor flow cell (bottom right) assembled with 10 nylon bolts and nuts. The liquids at the exit of the cell are collected into small beakers, the gas products instead are injected into the GC through a valve which is not showed in the picture. Also the powering system (solar panel + DC/DC regulator) is not visible in the picture.
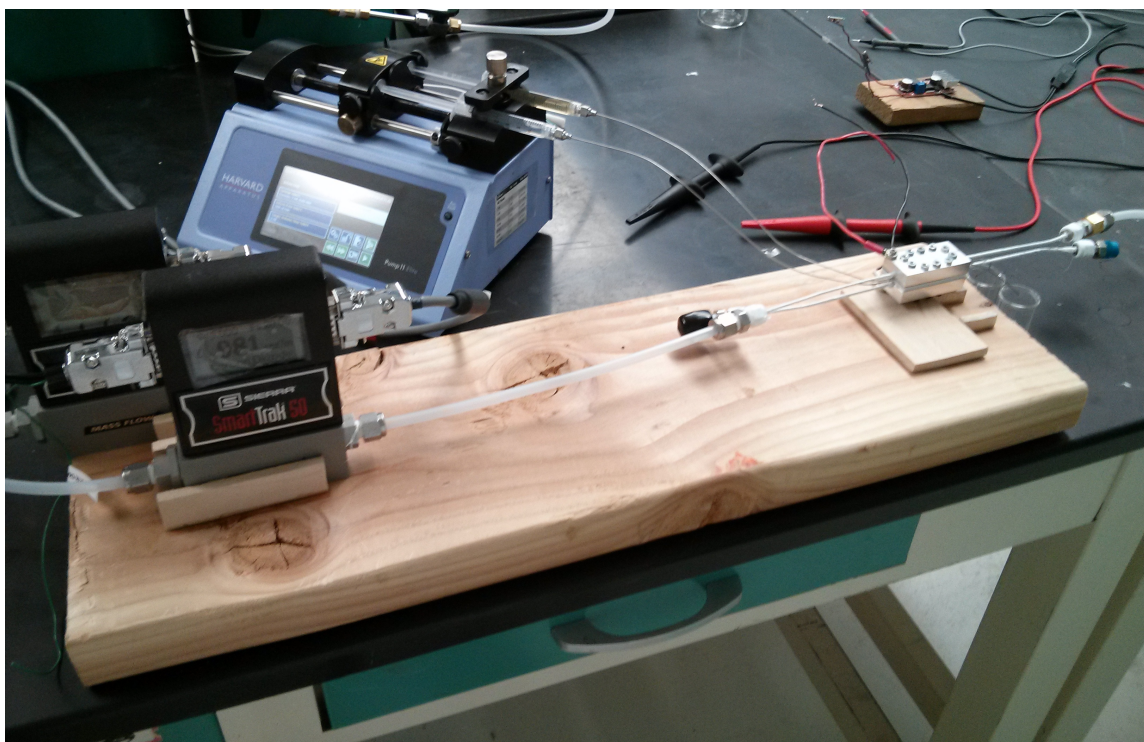
Figure 20. Picture of the actual setup.

4.4 Results and discussion

After the microfluidic reactor had been assembled, it was tested to verify the operating conditions. No relevant gas or liquid leakages were detected. An initial cell potential of 4 V was applied by the potentiostat in CA mode. At first, the reactor showed an overall non-stable response to the external power, with the cathode potential fluctuating between -1.0 V and -2.2 V vs. silver wire and current density fluctuating between 30 mA/cm^2 and 60 mA/cm^2. The large gap between the applied cell potential

and the cathode potential was attributed to losses in the system, such as membrane resistivity and ohmic potential drop in the electrolyte. The non-stability behavior was instead attributed to the high concentration of water present in the catholyte (96 mol% H_2O), which could have avoided the ionic liquid molecules to interact with the catalyst surface for the preliminary formation of the EMIM-complex (Equation 4.1), favoring water-splitting and hydrogen formation. This motivated the use of a solution with a lower concentration of water (90 mol% H_2O). According to experiments carried out in the three-electrode electrochemical cell at this solution concentration, the catalyst activity in terms of conversion rate (current density) was expected to decrease about 30 %, but still exhibit a greater current density for CO_2 reduction than what is reported in literature. Indeed, by applying the same cell potential (4 V), the reactor showed a stable behavior with steady cathode potential at -1.6 V and steady current density at 40 mA/cm^2. After 10 minutes, a 1 mL sample was injected into the GC for detection. The H_2 peak and CO peak were clearly visible at 1.8 min. and 8.8 min. of detection, respectively (Figure 20). Oxygen and Nitrogen were also detected due to the presence of a small amount of air in the tube connections as well as in the valve used for injecting the sample. It must be made clear that having bigger peak areas for O_2 and N_2 with respect to CO and H_2 does not mean that in the sample injected for detection the actual amount of air molecules was higher than the amount of syngas molecules. Only after calibration of the Gas Chromatograph for the different gases will be possible to judge about the actual volume composition of the sample.

For comparison, the system was run again but substituting the MoS_2 catalyst with an Ag catalyst (Ag NPs, 100 nm av. dia.) at the cathode. It was observed a similar GC detection curve trend, but with CO peak areas at least 3 times smaller than MoS_2 case. Similar results were obtained also changing the cell potentials from 4 V to 3.5 V and 3 V.
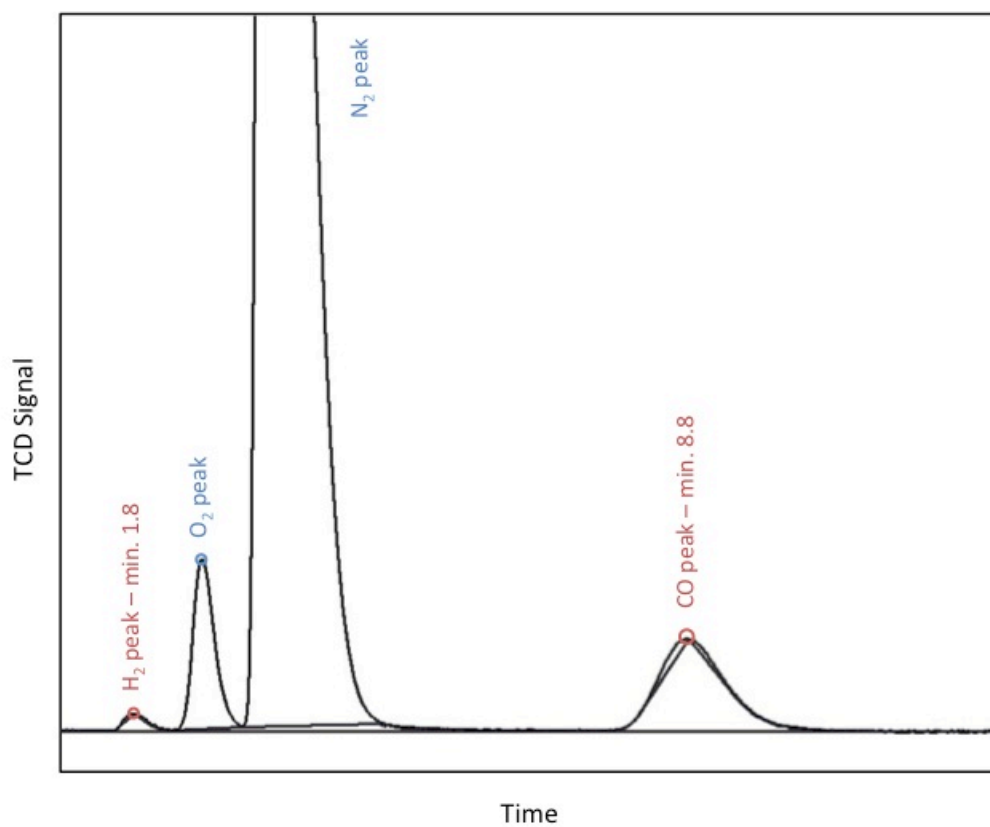

Figure 21. Peaks of gases detected by GC.

4.5   **Conclusion and future work**

The results obtained are promising. The MoS_2 catalyst showed excellent performance for CO_2 reduction in a batch electrochemical process in terms of overpotential, current efficiency, and current density. Its integration in a continuous-flow electrochemical cell produced excellent preliminary results. As expected, the microfluidic reactor was capable of continuously converting CO_2 into syngas in a heavily diluted electrolyte at high current density.

The use of this reactor is the first step for the development of a greener and more flexible substitute of traditional methods for syngas production. Syngas it is currently mainly manufactured through gasification of fossil based carbonaceous materials, in which coal is injected in high-pressure gasifiers that at high temperatures (>700°C) produce the constituting gas mixture of syngas. Although the gasification is well known and several plants already operate at industrial scale, production of syngas through gasifiers is still an under-development and high-cost technology.

The use of reactors that convert CO_2 into syngas can represent a valuable, energy-favorable, and environmental-friendly method for production of syngas. To test whether this system can compete in terms of energy efficiency and production rate, two steps would be eventually accomplished. First, the overall efficiency would be improved thanks to minimization of the losses inside the single cell. Subsequently, a scaling-up of

the system would be performed in order to reach a significant production rate (in terms of gas products flow rate). The scaling-up can be achieved either increasing the sizes of a single reactor (e.g. allowing a $10cm^2$ window for the catalyst in contact with the catholyte instead of a the actual $2cm^2$) or using a stack of multiple reactors together.

It must be said that the cell potential applied is still too high for the system to represent an energy-efficient and competitive setup for fuel production by CO_2 reduction. Further improvements of the cell, such as minimization of the losses associated to the ion-exchange membrane, total removal of leakages, and optimization of the cell design, would lower the potential needed for conversion, enhancing the overall energy efficiency. A possible solution for efficiency improvement could be the substitution of the anode catalyst material. As previously mentioned, the use of platinum nanoparticles results in the necessary separation of catholyte from anolyte (due to platinum poisoning) and the consequent utilization of a proton-exchange membrane. These represent main factor of losses and un-efficiency on the system. A catalyst material that does not get poisoned by the gas products of the reaction would permit the direct utilization of ionic liquid as electrolyte without the need of a second liquid channel for sulfuric acid and a separation technique. Graphite is a potential candidate to substitute platinum as electrode in the continuous-flow electrochemical cell for syngas production.

CITED LITERATURE

1 Halmann, M.M.: Chemical Fixation of Carbon Dioxide: Methods for Recycling CO2 into Useful Products. *CRC Press*, 1993.

2 Bennington, J.B.: The Carbon Cycle and Climate Change. *Brooks/Cole*, 2009.

3 Metz, B., Davidson, O.R., Bosch, P.R., Dave, R., and Meyer, L.A.: Climate Change 2007: Mitigation. Contribution of Working Group III to the Fourth Assessment Report of the Intergovernmental Panel on Climate Change. *IPCC*, Cambridge, United Kingdom and New York, 2007.

4 Schimel, D.S.: Recent patterns and mechanism of carbon exchange by terrestrial ecosystem. *Nature*, 414 (2001), 169-172.

5 Ballantyne, A.P., Alden, C.B., Miller, J.B., Tans P.P., and White J.W.C.: Increase in observed net carbon dioxide uptake by land and oceans during the past 50 years. *Nature*, 488 (2012), 70-72.

6 Friedlingstein, P.: Climate–Carbon Cycle Feedback Analysis: Results from the C4MIP Model Intercomparison. *Journal of Climate*, 19, 14 (2006).

7 Alexander, D.E. and Fairbridge, R.W.: Encyclopedia of Environmental Science, 2006.

8 Pachauri, R.K., and Reisinger, A.: IPCC, 2007: Climate Change 2007: Synthesis Report. Contribution of Working Groups I, II and III to the Fourth Assessment Report of the Intergovernmental Panel on Climate Change. *IPCC*, Geneva, Switzerland, 2007.

9 Kort, E.A., Wofsy, S.C., Daube, B.C., Diao, M., Elkins, J.W., Gao, R.S., Hintsa, E.J., Hurst, D.F., Jimenez, R., Moore, F.L., Spackman, J.R., and Zondlo, M.A.,: Atmospheric observations of Arctic Ocean methane emissions up to 82° north. *Nature Geoscience*, 5 (2012), 318-321.

10 Ineson, S., Scaife, A.A., Knight, J.R., Manners, J.C., Dunstone, N.J., Gray, L.J., and Haigh J.D.: Solar forcing of winter climate variability in the Northern Hemisphere. *Nature Geoscience* , 4 (2011), 753-757.

11 Hsu, K.J., Perry, C.A.: Geophysical, archaeological, and historical evidence support a solar-output model for climate change. *PNAS*, 97 (2000), 12433.

12 Arrhenius, S.: On the Influence of Carbonic Acid in the Air upon the Temperature of the Ground. *Philosophical Magazine and Journal of Science*, 41 (1896), 237-276.

13 Earth System Research Laboratory, Global Monitoring Division. *http://www.esrl.noaa.gov/gmd/ccgg/trends/*.

CITED LITERATURE (continued)

14 Palmer, P.N., and Pearson, M.R.: Atmospheric carbon dioxide concentrations over the past 60 million years. *Nature*, 406 (2000), 695-699.

15 CDIAC. Carbon Dioxide Information Analysis Center. http://cdiac.ornl.gov/#.

16 Canadell, J.G.: Contributions to accelerating atmospheric CO2 growth from economic activity, carbon intensity, and efficiency of natural sinks. *PNAS*, 104 (2007), 18866.

17 Raupach, M.R.: Global and regional drivers of accelerating CO2 emissions. *PNAS*, 104 (2007), 10288.

18 National Aeronautics and Space Administration, Goddard Institute for Space Studies.

19 Nakicenovic, N., Alcamo, J., Davis, G., Vries, B., Fenhann, J., Gaffin, S., Gregory, K., Grübler, A., and Jung, T.Y.: Emissions Scenarios. *IPCC,* Geneva, Switzerland, 2000.

20 Third Assessment Report "Climate Change 2001". *IPCC*, Geneva, Switzerland, 2001.

21 World Energy Outlook. *International Energy Agency,* Paris, France, 2006.

22 Global Carbon Budget. *http://www.globalcarbonproject.org/index.htm.*

23 Martinot, E.: *Renewable 2005, Global Status Report.* The Worldwatch Institute, 2005.

24 Metz, B.: Ogunlade Davidson, Heleen de Coninck. *Special Report on Carbon Dioxide Capture and Storage.* IPCC, 2005.

25 Jennifer, W.: *Carbon Capture.* Springer, 2012.

26 http://carma.org/plant/detail/29100.

27 House, K.Z., Baclig, A.C., Ranjan, M., van Nierop, E.A., Wilcox, J., Herzog, H.J.: Economic and energetic analysis of capturin CO2 from ambient air. *Proc. Natl. Acad. Sci.* , 108, 51 (2011), 20428.

28 Lightfoot, E.N., Cockrem, M.C.M.: What are dilute solutiones?. *Separ. Sci. Technol.*, 22 (1987), 165.

29 Direct Air Capture of CO2 with chemicals. *The American Physical Society*, 2011.

30 Biomass with CO2 Capture and Storage (Bio-CCS). *European Technology Platform for Zero Emission Fossil Fuel Power Plants.*

31 Carbon Sequestration Technology Roadmap and Program Plan. *U.S. Department of energy, Office of fossil energy, National Energy Technology Laboratory,* 2007.

32 Borowitzka., M.A.: Commercial production of microalgae: ponds, tanks, tubes and fermenters. *Journal of Biotechnology*, 70 (1999), 313.

33 Becker, E.W.: Microalgae: Biotechnology and microbiology. *Cambridge University* Press, USA, 1994.

CITED LITERATURE (continued)

34 DuBois, D.L.: Carbon. Electrochemical reactions of carbon dioxide. *Encyclopedia of Electrochemistry*, 7a (2006), 202.

35 Gattrell, M., Gupta, N., and Co, A.: A review of the aqueous electrochemical reduction of CO2 to hydrocarbons at copper. *Journal of Electroanalytical Chemistry*, 549 (2006), 1.

36 Hory, Y.: CO2 catalyzed at metal electrodes. *Handbook of Fuel Cells - Fundamental, Technology, and Applications*, 2 (2003), 720.

37 Sanchez-Sanchez, C.M., Montiel, V., Tryk, D.A., Aldaz, A., and Fujishima, A.: Electrochemical approaches to alleviation of the problem of carbon dioxide accumulation. *Pure and Applied Chemistry*, 73 (2001), 1917.

38 Carbon Dioxide Utilization, Electrochemical Conversion of CO2 – Opportunities and Challenges. *DNV*, 2011.

39 Basic research needs catalysis for energy, *PNNL 17214*. U.S. Department of Energy, 2007.

40 Paik, W., Andersen, T.N., and Eyring, H.: Kinetic studies of the electrolytic reduction of carbon dioxide on the mercury electrode. *Electrochimica Acta*, 14, 12 (1969), 1217.

41 Chandrasekaran, K., Bockris, L.O'M.: In-situ spectroscopic investigation of adsorbed intermediate radicals in electrochemical reactions: CO2− on platinum. *Surface Science*, 185, 3 (1987), 495.

42 Benson, E.E., Kubiak, C.P., Sathrum, A.J., and Smieja, J.M.: Electrocatalytic and homogeneous approaches to conversion of CO2 to liquid fuels. *Chem. Soc. Rev*, 38 (2009), 89.

43 Arakawa, H., Aresta, M., Armor, J.N., Barteau, M.A., Beckman, E.J., Bell, A.T., Bercaw, J.E., Creutz, C., Dinjus, E., Dixon, D.A., Domen, K., DuBois, D.L., Eckert, J., Fujita, E., Gibson, D.H., Goddard, W.A., Goodman, D.W., Keller, J., Kubas, G.J., Kung, H.H., Lyons, J.E., Manzer, L.E., Marks, T.J., Morokuma, K., Nicholas, K.M., Periana, R., Que, L., Rostrup-Nielson, J., Sachtler, W.M., Schmidt, L.D., Sen, A., Somorjai, G.A., Stair, P.C., Stults, B.R., Tumas, W.: Catalysis research of relevance to carbon management: progress, challenges, and opportunities. *Chem. Rev.*, 101 (2001), 953.

44 Suzuki, S., Hory, Y.: *Bull. Chem. Soc. Jpn.*, 55 (1982), 660.

45 Hori, Y., Kikuchi, K., Murata, A., Suzuki, S.: Production of methane and ethylene in electrochemical reduction of carbon dioxide at copper electrode in aqueous hydrogen carbonate solution. *Chem. Lett.* (1986), 897.

46 Gattrell, M., Gupta, N., and MacDougall, B.: A review of the aqueous electrochemical reduction of CO2 to hydrocarbons at copper. *J. Electroanal. Chem.*, 594 (2006),

CITED LITERATURE (continued)

47 Gupta, N., Gattrell, M., MacDougall, B.: Calculation for the cathode surface concentrations in electrochemical reduction of CO2 in KHCO3. *J. Appl. Electrochem.*, 36 (2006), 161.

48 Kenis, P.J., Whipple, D.T.: *J. Phys. Chem. Lett.* , 1 (2010), 3451.

49 Hori, Y., Murata, A., and Takahashi, R.: *J. Chem. Soc.*, 85 (1989), 2309.

50 Hori, Y., Wakebe, H., Tsukamoto, T., Koga, O.: Electrocatalytic process of CO selectivity in electrochemical reduction of CO2 at metal electrodes in aqueous media. *Electrochimica Acta*, 39 (1994), 1833.

51 Kuhl, K.P., Cave, E.R, Abram, D.N., and Thomas F. Jaramillo*c New insights into the electrochemical reduction of carbon dioxide on metallic copper surfaces. *Energy Environ. Sci.*, 5 (2012), 7050.

52 Hori, Y., Yoshinami, Y., Kawarada., H.: Abstract of Annual Meeting of ISE (1990).

53 Ito, K., Murata, T., and Ikeda, S.: *Bull. Nagoya Inst. Techn.*, 27 (1975), 209.

54 Köleli, F., and Balun, D.: Reduction of CO2 under high pressure and high temperature on Pb-granule electrodes in a fixed-bed reactor in aqueous medium. *Applied Catalysis A: General*, 274, 237.

55 Hori, Y., Wakebe, H., Tsukamoto, T., and Koga, O.: Electrocatalytic process of CO selectivity in electrochemical reduction of CO2 at metal electrodes in aqueous media. *Electrichim. Act.*, 39 (1994), 1833.

56 Hori, Y., Kikuchi, K., and Suzuki, S.: Production of CO and CH4 in electrochemical reduction of CO2 at metal electrodes in aqueous hydrogencarbonate solution. *Chem. Lett.* (1985), 1695.

57 Noda, H., Ikeda, S., Oda, Y., Imai, K., Maeda, M., and Ito, K.: *Bull. Chem. Soc. Jpn.*, 63 (1990), 2459.

58 Yano, H., Shirai, F., Ogura. H.: *J. Electroanal. Chem.* , 533 (2002), 113.

59 Hori., Y.: Electrochemical CO2 Reduction on Metal Electrodes. In *Modern Aspect of Electrochemistry* (Vol.42).

60 Hoshi, N., Kato, M., Hori, Y.: Electrochemical reduction of CO2 on single crystal electrode of Ag(111), Ag(100) and Ag(110). *Journal of Electroanalytical Chemistry*, 440 (1997), 283.

61 Salehi-Khojin, A., Jhong, H.M, Rosen, B.A., Zhu, W., Ma, S., Kenis, P.J.A., and Masel, R.I.: Nanoparticle silver catalysts that show enhanced activity for carbon dioxide electrolysis. *The Journal of Physical Chemistry*, 117 (2013), 1627.

62 Ito, K., Ikeda, S., Takagi, T.: *Bull. Chem. Soc. Jpn.* , 60 (1987), 2517.

63 Feroci, M., Orsini, M., Rossi, L., Sotgiu, G., and Inesi, A.: *J. Org. Chem.*, 72 (2007), 200.

CITED LITERATURE (continued)

64 Barrosse-Antle, L.E, and Compton, R.G.: Reduction of carbon dioxide in 1-butyl-3-methylimidazolium acetate. *Chem. Commun.* (2009), 3744.

65 Zhang, L., Niu, D.F., Zhang, K., Zhang, G.R., Luo, Y.W., and Lu, J.X.: Electrochemical activation of CO2 in ionic liquid (BMIMBF4): synthesis of organic carbonates under mild conditions. *Green Chem.*, 10 (2008), 202.

66 Zhao, G., Jiang, T., Han, B., Li, Z., Zhang, J., Liu, Z., He, J., and Wu, W.: Electrochemical reduction of supercritical carbon dioxide in ionic liquid 1-n-butyl-3-methylimidazolium hexafluorophosphate. *The Journal of Supercritical Fluids*, 32 (2004), 287.

67 Fenga, Q., Liua, S., Wanga, X., and Jina, G.: Nanoporous copper incorporated platinum composites for electrocatalytic reduction of CO2 in ionic liquid BMIMBF4. *Applied Surface Science*, 258 (2012), 5005.

68 Rosen, B.A., Salehi-Khojin, A., Thorson, M.R., Zhu, W., Whipple, D.T., Kenis, P.J.A., and Masel, R.I.: Ionic Liquid-Mediated Selective Conversion of CO2 to CO at low overpotentials. *Science*, 334 (2011), 643.

69 Energy efficiency and renewabpe energy alternative fuels data center. *U.S Department of Energy*.

70 Karunadasa, H.I.: A Molecular MoS2 Edge Site Mimic for Catalytic Hydrogen Generation. *Science*, 335 (2012), 698.

71 Rosen, B.A., Zhu, W., Kaul, G., and Masel, R.I.: Water Enhancement of CO2 Conversion on Silver in 1-Ethyl-3-Methylimidazolium Tetrafluoroborate. *Journal of the Electrochemical Society*, 160 (2013), H138.

72 Yamamoto, T., Tryk, D.A., Fujishima, A., and Ohata, H.: Production of syngas plus oxygen from CO2 in a gas-diffusion electrode-based electrolytic cell. *Electrochim. Acta*, 47 (2002), 3327.

73 Delacourt, C., Ridgway, P.L., Kerr, J.B., and Newman, J.: Design of an Electrochemical Cell Making Syngas (CO + H2) from CO2 and H2O Reduction at Room Temperature Fuel Cells and Energy Conversion. *J. Electrochem. Soc.*, 155 (2008), B42.

74 Rosen, B.A., Haan, J.L., Mukherjee, P., Braunschweig, B., Zhu, W., Salehi-Khojin, A., Dlott, D.D., and Masel, R.I.: In Situ Spectroscopic Examination of a Low Overpotential Pathway for Carbon Dioxide Conversion to Carbon Monoxide. *The Journal of Physical Chemistry*, 116 (2012), 15307.

VITA

Name: Davide Pisasale

Education: B.S., Mechanical Engineering, Politecnico di Torino, Turin, Italy, 2011

M.S., Mehcanical Engineering, Politecnico di Torino, Turin, Italy, 2013

M.S., Mechanical Engineering, University of Illinois at Chicago, Chicago, Illinois, 2013

Experience: Graduate Research Assistant at the Nanomaterials and Energy System Laboratory, Prof. Salehi-Khojin, Department of Mechanical and Industrial Engineering, UIC, Chicago, Illinois. 2012-2013

Honors: Recipient of TOP-UIC mobility scholarship for Double Degree program between Politecnico di Torino and University of Illinois at Chicago.